

**Forschungszentrum Karlsruhe**  
Technik und Umwelt

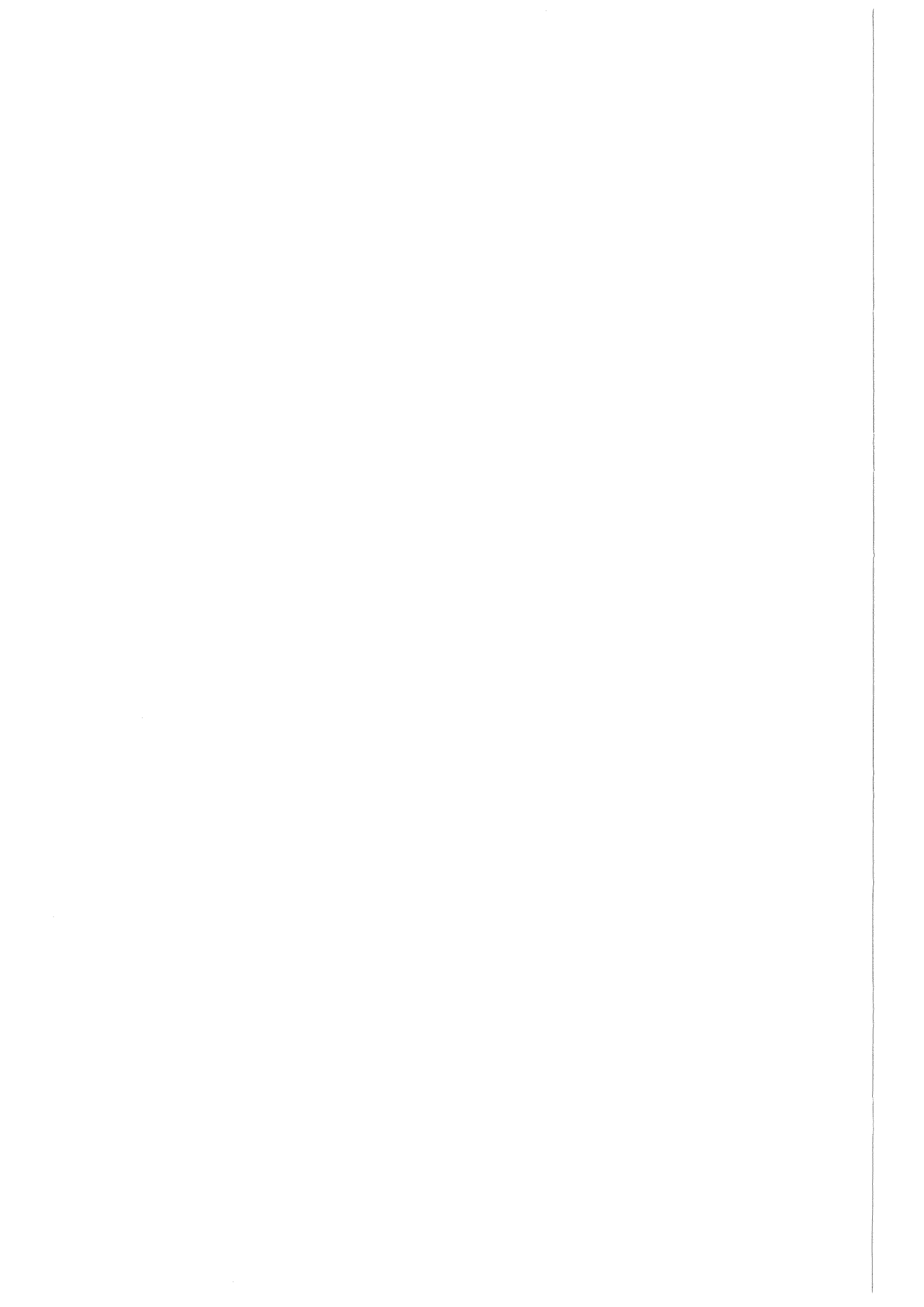
**Wissenschaftliche Berichte**  
FZKA 6338

**FZK Contribution to the ESIS  
TC8 Numerical Round Robin  
on Micromechanical Models  
Phase II  
Task B1**

**H. Riesch-Oppermann**  
Institut für Materialforschung  
Projekt Kernfusion

**September 1999**

---



**Forschungszentrum Karlsruhe**  
Technik und Umwelt  
Wissenschaftliche Berichte  
FZKA 6338

FZK Contribution to the ESIS TC 8  
Numerical Round Robin on Micromechanical Models  
Phase II  
Task B1

H. Riesch-Oppermann  
Institut für Materialforschung  
Projekt Kernfusion

Forschungszentrum Karlsruhe GmbH, Karlsruhe

1999

**Als Manuskript gedruckt**  
**Für diesen Bericht behalten wir uns alle Rechte vor**

**Forschungszentrum Karlsruhe GmbH**  
**Postfach 3640, 76021 Karlsruhe**

**Mitglied der Hermann von Helmholtz-Gemeinschaft**  
**Deutscher Forschungszentren (HGF)**

**ISSN 0947-8620**

## Abstract

Within the European Structural Integrity Society (ESIS), a Round Robin was launched by the *Technical Committee 8: Numerical Methods* with the objective to establish reproducible numerical procedures for the identification of parameters for numerical modelling of ductile and cleavage failure. A ferritic steel with the German designation of 22 NiMoCr 3 7 was chosen as reference material. The present report contains the results of the FZK contribution to Phase II, Task B1 of the Round Robin, which is aimed at the identification of cleavage fracture parameters from the numerical analysis of notched tensile specimen cleavage fracture data. The results comprise deformation behaviour, Weibull stress at fracture, and statistical parameters of the critical Weibull stress including confidence intervals. The FZK code WEISTRABA [1] was employed for the calculations. The results are obtained for a subset of the specimens as well as for the complete data set, because some scatter in the load-displacement records up to fracture was observed. Novel statistical techniques were used to obtain confidence intervals for the distribution parameters of the Weibull stress at fracture by stochastic simulation. These techniques also provide information about the joint statistical distribution of the estimates for the distribution parameters which, in turn, indicate whether the statistical methods used are indeed applicable in this particular case.

## Zusammenfassung

### **Numerischer ESIS-Round Robin: Mikromechanische Modelle; Phase II, Task B1**

Innerhalb eines numerischen Round Robins, der vom Technischen Ausschuss 8 (Numerische Methoden) der Europäischen Gesellschaft für strukturelle Integrität (ESIS) angeregt wurde, soll auf Grundlage einer Datenbasis für den Referenzwerkstoff 22 NiMoCr 3 7 die Reproduzierbarkeit numerischer Auswerteverfahren zur Ermittlung der Parameter für mikromechanische Modelle zur Beschreibung des spröden und duktilen Versagensverhaltens ferritischer Stähle untersucht werden. Der vorliegende Bericht enthält den Beitrag des FZK zur Aufgabe B1 innerhalb der Phase II dieses Round Robins, nämlich die Identifizierung der Spaltbruchparameter aus den Ergebnissen an Zugversuchen mit gekerbten Rundzugproben. Die Ergebnisse umfassen sowohl die Beschreibung des Deformationsverhaltens als auch die daraus gewonnenen Werte der Weibullspannung beim Bruch und die Bestimmung der statistischen Parameter der Weibullspannung beim Bruch einschließlich der entsprechenden Konfidenzintervalle. Die statistische Auswertung wurde mit dem am FZK entwickelten Programmsystem WEISTRABA [1] durchgeführt. Aufgrund von beobachteten Abweichungen im Kraft-Verformungsverhalten wurde die Analyse sowohl für einen ausgewählten Teil mit relativ kleinen Abweichungen als auch für den gesamten Satz der getesteten Proben durchgeführt. Zusätzlich zu den üblicherweise angewandten Verfahren wurden neue stochastische Methoden eingesetzt, die auf Simulationsmethoden basieren und sowohl die Ermittlung von Konfidenzintervallen für die Verteilungsparameter als auch von Konfidenzbereichen für die statistische Verteilung der Weibullspannung selbst erlauben. Darüberhinaus liefern sie Informationen über die gemeinsame statistische Verteilung der Schätzer für die Verteilungsparameter selbst und damit wichtige Hinweise über die Tragfähigkeit der eingesetzten statistischen Methoden.

# Contents

<b>1</b>	<b>Introduction</b>	<b>1</b>
<b>2</b>	<b>Procedure</b>	<b>3</b>
2.1	FE specifications and meshing . . . . .	3
2.2	Analysis of reference load cases . . . . .	3
2.3	"Layer 4" stress / displacement analysis . . . . .	4
2.4	Weibull stress analysis . . . . .	4
2.4.1	Weibull stress calculation . . . . .	4
2.4.2	Maximum likelihood procedure . . . . .	5
2.4.3	Use of advanced statistical methods . . . . .	6
<b>3</b>	<b>Reporting of the results</b>	<b>9</b>
3.1	FE meshing . . . . .	9
3.2	FE code & algorithms . . . . .	9
3.3	Cleavage fracture models . . . . .	9
3.4	Stress averaging procedure . . . . .	9
3.5	Load vs. reduction of diameter calculation . . . . .	10
3.6	Table of local quantities . . . . .	10
3.7	$\sigma_W$ -results for $m = 22$ . . . . .	10
3.8	Weibull parameter estimation results . . . . .	10
3.9	Global quantities . . . . .	10
3.10	Comments . . . . .	11
3.11	Modelling of the complete set of $N = 32$ specimens . . . . .	11
3.12	Results . . . . .	12

<b>4</b>	<b>Beneficial use of bootstrap simulations</b>	<b>13</b>
4.1	Background and procedure . . . . .	13
4.1.1	Basic idea of bootstrapping . . . . .	14
4.1.2	Bootstrap confidence intervals . . . . .	14
4.2	Results . . . . .	15
4.2.1	Weibull stress bootstrapping procedure . . . . .	15
4.2.2	Bootstrap results for parameter estimation . . . . .	16
4.2.3	Bootstrap results for confidence intervals . . . . .	16
4.2.4	Bootstrap results for probabilities . . . . .	17
<b>5</b>	<b>Summary and conclusions</b>	<b>19</b>
	<b>References</b>	<b>21</b>
<b>A</b>	<b>Scheme of the iterative maximum likelihood procedure</b>	<b>23</b>
<b>B</b>	<b>Figures and Tables</b>	<b>25</b>
<b>C</b>	<b>Task Description</b>	<b>39</b>

# List of Figures

A.1	Flow diagram for the iterative Weibull parameter estimation procedure . . .	24
B.1	Meshing of the specimen . . . . .	25
B.2	Detail of specimen meshing at the notch root . . . . .	26
B.3	Axial stress distribution along $z = 0$ . . . . .	26
B.4	Distribution of equivalent plastic strain along $z = 0$ . . . . .	27
B.5	Simulation of notched specimen contraction . . . . .	27
B.6	$F - \Delta D$ records of all tested specimens in the ESIS Round Robin . . . . .	28
B.7	Weibull stress results for all specimens compared to results for layer 4 . . .	28
B.8	Bootstrap results for layer 4 . . . . .	29
B.9	Bootstrap results for all specimens . . . . .	29
B.10	Bootstrap results for layer 4 and all specimens compared . . . . .	30
B.11	Bootstrap confidence intervals of $m$ for layer 4 . . . . .	30
B.12	Bootstrap confidence intervals of $m$ for all specimens . . . . .	31
B.13	Bootstrap confidence intervals of $\sigma_u$ for all specimens . . . . .	31
B.14	Bootstrap confidence intervals of $m$ for layer 4 and all specimens compared	32
B.15	CDF bootstrap and ML confidence intervals (layer 4) . . . . .	32
B.16	Influence of bootstrap size on bootstrap confidence intervals . . . . .	33
B.17	CDF bootstrap confidence intervals for layer 4 and all specimens . . . . .	33



# List of Tables

B.1	Force and diameter contraction of FE calculation at reference steps . . . . .	34
B.2	Local quantities for layer 4 specimens . . . . .	35
B.3	Global quantities for layer 4 specimens. . . . .	35
B.4	Global quantities (all spec's). . . . .	36
B.5	Ranking of specimens and corresponding layers . . . . .	37
B.6	Maximum likelihood and bootstrap confidence intervals (layer 4) . . . . .	37
B.7	Maximum likelihood and bootstrap confidence intervals (all specimens) . . . . .	37



# Introduction

The present analysis is part of the **European Structural Integrity Society (ESIS) - Numerical Round Robin on Micromechanical Models**. It is related to the present Phase II of the Round Robin, **Numerical simulation of fracture mechanics tests, Task B1 Cleavage fracture of notched tensile bars**.

The preceding Phase I of the Round Robin concentrated on the simulation of standard smooth and notched tensile bar specimens and the identification of critical damage parameters for ductile tearing at room temperature and for cleavage fracture at  $-196^{\circ}\text{C}$  [2].

Some of the results of Phase I had to be re-evaluated in Phase II due to an extension of the underlying database. This was done under Tasks A1 and B1 of Phase II.

The following Phase III is intended to model fracture mechanics tests to predict the fracture toughness behaviour in the ductile-to-brittle transition regime.

Evaluation procedures for the parameters of the Weibull stress at the onset of cleavage fracture for notched round bar specimens are compared within the present Task B1.

The procedure requires some non-standard techniques in different fields of engineering knowledge. Advanced continuum mechanics stress analysis is combined with non-standard approaches for the statistical evaluation of the results. Statistical inference is used to assess the uncertainty of the results and to draw conclusions regarding the significant differences between different data sets. For the evaluation of the local approach fracture parameters, a hybrid technique is applied using experimentally determined fracture data and adapting numerical results before evaluating them statistically. Results of the Round Robin are felt to contribute to revealing the impact of differences in numerical analysis, statistical evaluation, or data processing strategies pursued by the various participants. The results obtained will give confidence of or allow for an appropriate modification of the ESIS P6 procedure [3] for the determination of local approach cleavage fracture parameters.

The FZK contribution to the Round Robin is described in the sequel where the procedure was split up into different steps.

First, a stress / displacement analysis is performed using three given reference load cases "1", "2", and "3" with prescribed imposed axial displacements as specified in the task description.

Second, the stress field at fracture was calculated. The corresponding parameters of the Weibull stress were then determined according to the ESIS P6 procedure [3] and using the WEISTRABA [1] code.

Following the suggestions of the task description, the analysis was, in a first step, restricted to the 7 specimens in the so-called "layer 4". A statistical evaluation of the Weibull stress is of somewhat limited value due to the very small number of tested specimens, and the results are mainly useful to check and compare the different numerical procedures involved and used by the different participants of the Round Robin. Therefore, the analysis of the fracture stress for the entire set of specimens was performed in a second step. Some remarks are given finally on the scatter in the load-deformation behaviour of specimens resulting from different locations (i.e. different "layers") of the forged ring segment from which the specimens were obtained.

The report is completed by a Section containing some results of a novel statistical evaluation procedure for the assessment of uncertainties in the statistical inference of distribution parameters using so-called bootstrap or resampling methods. It is felt that especially in the present case, where the random variable, namely the Weibull stress, depends on the (unknown) value of one distribution parameter, these methods overcome the inherent limitations of the ordinary maximum-likelihood procedure.

# Procedure

This report covers the FZK contribution to the analyses for task B1. In the following Sections, meshing of the specimen, stress / displacement analyses, and  $\sigma_W$ -analyses are presented.

If not stated otherwise, all stresses are given in MPa, lengths are in mm, and strains are dimensionless.

## 2.1 FE specifications and meshing

The general purpose Finite Element code ABAQUS [4] was used throughout these Round Robin calculations. An axisymmetric 2-D model of the simplified notched round bar geometry as specified in the task description was set up and is shown in Fig. B.1. Only one half of the specimen was modelled for symmetry reasons. The model contains 496 elements and 1585 nodes. Axisymmetric isoparametric quadratic CAX8R-elements with 8 nodes and reduced integration were used. ABAQUS large displacement analysis was performed for all calculations. The element size at the notch root was  $0.065 \times 0.130 \text{ mm}^2$ . There were 18 elements in the fracture plane at  $z = 0$ .

The element size and the reference volume  $V_0$  are chosen independently in subsequent calculations. In fact,  $V_0$  only serves as a reference volume for dimensional purposes and hereinafter is set to  $V_0 = 1 \text{ mm}^3$ .

Boundary conditions due to symmetry were:

$$u_z = 0 \quad \text{at} \quad z = 0 \quad \text{and} \quad u_r = 0 \quad \text{at} \quad r = 0 \quad (2.1)$$

Loading was applied by prescribed  $z$ -displacement boundary conditions for the nodes at  $u_z = 28$ .

The external force,  $F$ , was calculated from the axial stresses at  $u_z = 28$ .

## 2.2 Analysis of reference load cases

A conventional large displacement elasto-plastic analysis was performed using the stress / strain data given in the task description for a piecewise linear approximation of the true stress - true strain input for ABAQUS.

According to the task description, the yield stress  $R_{eL}$  was 720 MPa with  $R_{eL}/E = 0.00338028$  and a Young's modulus of  $E = 213.000$  GPa. Poisson's ratio was set to  $\nu = 0.3$ . The stress-strain law was given by  $\ln(\sigma/\text{MPa}) = 0.16824 \ln \epsilon + 7.206$  for a true stress of  $\epsilon \geq 0.03$ .

For the stress / displacement analysis of the reference steps designated "1", "2", and "3", the prescribed  $z$ -displacement boundary conditions for the nodes at  $u_z = 28$  were .1mm, .2mm, and .3mm, respectively. A complete  $F - \Delta D$  curve containing the reference steps was generated from the FE results in order to facilitate the "layer 4" stress and displacement analysis for the Weibull stress evaluation.

Plots of the axial stress and the equivalent plastic strain distribution along the  $z$ -symmetry line  $z = 0$  were generated. They give some overall information about the mechanical conditions in the specimen.

## 2.3 "Layer 4" stress / displacement analysis

For the stress / displacement analysis of the "layer 4" specimens at fracture, the  $z$ -displacement boundary conditions for the nodes at  $u_z = 28$  were determined from the  $F - \Delta D$  curve of the reference steps. Iterative adaptation of the displacement boundary conditions at  $u_z = 28$  was necessary to meet the  $\Delta D$ -values at fracture with sufficient accuracy and to avoid interpolation between subsequent load steps.

## 2.4 Weibull stress analysis

The Weibull stress at cleavage fracture is a random variable that characterizes the fracture resistance of the material against cleavage (brittle) fracture.

### 2.4.1 Weibull stress calculation

The Weibull stress  $\sigma_W$  is defined by

$$\sigma_W^m = \frac{1}{V_0} \int_{V_{pl}} \sigma_1^m dV \quad (2.2)$$

where  $m$  is the so-called Weibull slope,  $V_0$  is a reference volume,  $V_{pl}$  is the volume of the plastic zone, and  $\sigma_1$  is the first principal stress.

The statistical distribution of its critical value, i.e. the value at cleavage fracture, is given by

$$F_{\sigma_W}(\sigma_W) = 1 - \exp\left(-\left(\frac{\sigma_W}{\sigma_u}\right)^m\right) \quad (2.3)$$

The distribution parameters  $\sigma_u$  and  $m$  of the Weibull stress  $\sigma_W$  at fracture are determined by the maximum likelihood procedure as given in [3].

For numerical reasons, the integration of the Weibull stress according to eq. (2.2) is performed after normalizing  $\sigma_1$  by a suitably chosen reference stress, e.g. the flow stress. This is done to avoid numerical difficulties resulting from large values of the Weibull exponent  $m$  which is typically in the range of 10-30. The correction is removed after the numerical integration has been completed. Eq. (2.2) then reads:

$$\left(\frac{\sigma_W}{\sigma_{\text{ref}}}\right)^m = \frac{1}{V_0} \int_{V_{pl}} \left(\frac{\sigma_1}{\sigma_{\text{ref}}}\right)^m dV \quad (2.4)$$

and final adjustment is simply made by multiplying the resulting integral value by the value of the reference stress  $\sigma_{\text{ref}}^m$ .

The first principal stress values at the integration points of the ABAQUS elements are obtained with the help of a post-processing routine [1]. If reduced integration is used, which means that we have  $2 \times 2 = 4$  integration points per element in the 2D case, integration of the Weibull stress can be re-written as the sum over the elements

$$\begin{aligned} \sigma_W &= \sigma_{\text{ref}} \left[ \frac{1}{V_0} \sum_{\text{el}} \sigma_{W_{\text{el}}} \right]^{\frac{1}{m}} \quad \text{with} \\ \sigma_{W_{\text{el}}} &= \sum_{i=1}^{k_i} w_i \sum_{j=1}^{k_j} w_j \left( \frac{\sigma_1(r_i, s_j)}{\sigma_{\text{ref}}} \right)^m (\det J(r_i, s_j)) \end{aligned} \quad (2.5)$$

with  $k_i, k_j$  denoting the number of integration points in each dimension and  $w_i, w_j$  being the respective weights of the Gauss quadrature. Det  $J$  is the determinant of the mapping to the natural element coordinates. An appropriate symmetry factor has to be applied. In the present axisymmetric 2-D analysis the symmetry factor is  $2 * 2\pi$ , as the total volume of the specimen is twice that of the model.

A plastic zone indicator flag (in terms of a von Mises yield criterion) is used to extend numerical integration over the plastic zone only and not over the entire volume of the specimen. Any stress averaging procedures are avoided.

For each FE load step, corresponding to a specimen fracture event, the first principal stress values are checked against the values of the previous step and a stress envelope is constructed to take into account locally decreasing stresses due to stress redistribution which might otherwise lead to decreasing values of the local risk of rupture. This stress envelope containing the maximum of the first principal stress at each node is used for the calculation of the Weibull stress.

## 2.4.2 Maximum likelihood procedure

The determination of the two parameters  $m$  and  $\sigma_u$  has to be performed iteratively as  $\sigma_W$  depends on the (unknown) parameter  $m$ . The WEISTRABA post-processor developed at FZK was used [1] in accordance with the procedure fully described in ESIS P6 [3]. For the sake of completeness, the essential steps are given in Appendix A.

Though the procedure does not rely on probability plotting except for visualization of the results, some remarks on probability plotting seem to be appropriate.

In the task description, it was suggested to use  $h_i = (i - 0.5)/n$  as plotting position for the cumulative fracture probability. We decided to choose instead  $h_i = i/(n + 1)$  as plotting position for the probability axis in the Weibull plot. This choice corresponds to the expectation value of the cumulative frequency [5] of the  $i$ -th value of an ordered sample of size  $n$ :  $\overline{F(x_{(i)})} = i/(n + 1)$  and is consistent with the ESIS P6 procedure.

However, as early as 1960, Kimball [6] noted:

... it is to be noted that the simplification afforded by the use of probability-scale graph paper is a *visual* simplification. ... If the approach is to be purely analytical, there is no point in using the special scale paper.

Thus, in case of the use of a maximum likelihood procedure, results are in no way affected by different choices for the definition of  $h_i$ . Nevertheless, the choice of  $h_i = i/(n + 1)$  is strongly recommended because of its well-known statistical properties<sup>1</sup> (at least in the case of non-iterative estimates).

### 2.4.3 Use of advanced statistical methods

It should be emphasized that the evaluation of the distribution parameters of  $\sigma_w$ , namely  $m$  and  $\sigma_u$ , is based on statistical inference methods that are applied without fully meeting the conditions of their applicability. It is not clear beforehand whether the maximum likelihood parameter estimation gives valid results for the present case, where the random variate depends on the distribution parameter itself and an iterative procedure is used to obtain consistent results. There are no methods available to quantify the statistical properties of the estimators of the Weibull parameters.

For these reasons, the confidence intervals based on the results found by Thoman et al. [7] and used in the ESIS P6 procedure [3] may only approximately reflect the statistical uncertainty of the parameter estimates. This situation is completely different from the Weibull parameter estimation in the strength measurement for ceramics, where no iterative procedure is required.

There are novel statistical techniques capable to reflect the complex behaviour of random variates because they are not based on parametric models: so-called bootstrap or resampling methods can be used to generate confidence intervals by simulation [8]. The parent distribution used for the simulation is the empirical distribution of the available experimental sample. The essential advantage over classical statistical inference methods is the fact that these methods use empirical distributions of statistical estimates for the generation of confidence intervals. Thus, there is no need to know the closed-form solution for the distribution of the statistical estimate as is the case in the classical methods. From a statistical point of view, this is equivalent to the use of non-parametric maximum-likelihood estimators instead of parametric maximum-likelihood estimators, for which the usual confidence intervals are generated [9].

Resampling methods are well-known in the field of medicine and biology, but only begin to enter in materials science [10], though there is some effort to base coding schemes on resampling ideas [11].

---

<sup>1</sup>also, the variance of the  $i$ -th frequencies is known:  $\sigma^2(F_{(i)}) = \frac{i(n-i+1)}{(n+2)(n+1)^2} = \frac{\overline{F_{(i)}}(1-\overline{F_{(i)}})}{n+2}$  [5]

In Chapter 4, results for parameter correlation and confidence intervals are given and compared with standard Weibull evaluation results.



# Reporting of the results

According to the task description which is given in Appendix C, results are presented in the suggested order within the following subsections:

## 3.1 FE meshing

The geometry of the FE mesh is shown in Fig. B.1. 8-noded axisymmetric isoparametric quadratic elements with reduced integration (ABAQUS designation: `CAX8R`) were used. 18 elements were located in the fracture plane at  $z = 0$  (see Fig. B.2). The notch root element size was  $0.065 \times 0.130 \text{ mm}^2$ . Only one half of the specimen was modelled due to symmetry.

## 3.2 FE code & algorithms

ABAQUS 5.7/5.8 was employed [4]. Elastic-plastic material behaviour was modelled using a Mises yield surface and isotropic hardening. Large strain analysis was used for all calculations. Updated Lagrange-Jaumann formulation is used by ABAQUS.

## 3.3 Cleavage fracture models

The Beremin model with no strain correction is used for the calculation of  $\sigma_W$  as described above. The iterative procedure for the determination of the parameters  $m$  and  $\sigma_u$  is described in Appendix A.

## 3.4 Stress averaging procedure

No stress averaging is performed. Gauss quadrature is applied with stresses at the integration points within each element using a plastic zone flag as described above.

### 3.5 Load vs. reduction of diameter calculation

The simulation results are tabulated in Table B.1 up to  $\Delta d = .6$  mm and shown in Fig. B.5.

### 3.6 Table of local quantities

Table B.2 contains the prescribed displacements at  $u_z = 28$  mm for the layer 4 specimens as well as some local quantities for stresses and plastic strains in the centre and the notch root elements, respectively.

Additional results are presented in Figures B.3 and B.4. Figure B.3 shows the axial stress distribution along a line  $z = 0$  from the specimen centre (left) to the notch root (right) for the three reference load cases. Figure B.4 shows the corresponding distribution of the equivalent plastic strains along the same line.

### 3.7 $\sigma_W$ -results for $m = 22$

Table B.3 shows the calculated Weibull stresses for an initial value for the Weibull modulus set to  $m = 22$ . This is considered to contain much more information than the  $\sigma_u$ -value alone. No confidence intervals are given for this case, because the confidence limits only apply to maximum likelihood estimates.

The value of  $\sigma_u$  after the first step was  $\sigma_u = 1839.9$  MPa; the value of  $m_{cor}$  calculated from the first iteration was  $m_{cor} = 42.5$ .

### 3.8 Weibull parameter estimation results

The final results of the Weibull parameter estimation procedure are also given in Table B.3. The iteration procedure converged after 3 iterations. The allowed difference of  $m_{cor}$  between two subsequent iterations was  $\Delta m = 0.1$ .

Final results were:  $m = 54.6$  and  $\sigma_u = 1706.9$  MPa.

Bias correction ( $N = 7$ ) gives  $m_{cor} = 43.2$ .

The symmetrical 90% confidence intervals for  $m$  and  $\sigma_u$  are:

$$25.0 \leq m \leq 77.0 \quad \text{and} \quad 1681.2 \text{ MPa} \leq \sigma_u \leq 1734.5 \text{ MPa}.$$

### 3.9 Global quantities

Table B.3 additionally contains the required global quantities for the prescribed values of the diameter reduction at fracture for the 'layer 4' specimens. These are the prescribed displacement  $u_z(z = 28)$  (calculated from the FE load-displacement curve) and the reaction force  $F$  (calculated from the nodal axial stress values  $\sigma_{zz}$  at  $z = 28$ mm).

Table B.3 also contains the sample of  $\sigma_W$ -values for the initial  $m = 22$  and for the final value of  $m$  after termination of the iteration procedure.

### 3.10 Comments

Due to the small sample size, the confidence intervals for  $m$  are quite large.

Convergence of the iterative ML-procedure was achieved after 3 steps using a starting value of  $m = 22$  and a tolerance of  $\Delta m = 0.1$ .

Interpretation of the results in terms of statistical inference seems to be of no value because of the small sample size. Interpretation of the results actually is only possible in terms of the numerical results and the accuracy of the numerical values obtained for the Weibull stress at fracture and its distribution parameters  $m$  and  $\sigma_u$ , respectively, from other Round Robin contributions.

Chapter 4 will reveal some specific features of the small sample estimation for  $m$  in this case.

### 3.11 Modelling of the complete set of $N = 32$ specimens

An attempt was made to evaluate the complete set of specimens and obtain results for the Weibull stress parameters. Figure B.6 shows the  $F - \Delta D$  records of all tested specimens. Considerable scatter in the load-displacement behaviour can be observed. However, a closer look on the data shows that the scatter is present within various layers, especially layers 5 and 6, whereas the scatter between the layers is not so pronounced, showing, however, a slight tendency of the force  $F$  to increase for fixed  $\Delta D$  from the inside layer 1 towards the outside layers 5 and 6.

Scatter of the load values for a given notch root displacement of  $\Delta D = 0.2\text{mm}$  is approximately  $\pm 3\%$ . The FE simulation meets the mean behaviour of all specimens quite well with some tendency to overestimate layer 1-3 forces and to (moderately) underestimate the layer 5-6 forces.

Considering that  $\Delta D$  is the essential parameter controlling fracture, it was decided to regard the observed scatter in the load-deformation characteristics as negligible.

The question that was raised in the task description with respect to ranking does not seem to pose any severe problems, because the ranking parameter for the statistical evaluation has to be  $\sigma_W$  and so the ranking problem only enters into the load step control of the FE analysis, but not into the evaluation process of the Weibull parameters. (Finally, if the maximum likelihood method is used, no ranking of the results is necessary at all!)

Proceeding that way, we finally end up with some kind of implicit scaling which is done by using a "mean" stress-strain curve and  $\Delta D$  as a control parameter for the fracture load and the stress distribution at fracture to be determined by FEM analysis.

Simple scaling of the stress field does not seem to be appropriate. Scaling could map the deformation curves of the different layers onto one average curve, but it would still not be able to reflect the non-linear behaviour of the plastic zone evolution.

## 3.12 Results

Table B.4 shows the results for the global quantities of the complete set of  $N = 32$  specimens. No table of local results was generated. The maximum likelihood estimates of the Weibull stress parameters were  $m = 20.9$  ( $m_{cor} = 20.0$ ) and  $\sigma_u = 1913.6$  MPa. The 90% maximum likelihood confidence intervals for  $m$  and  $\sigma_u$  are:

$$15.9 \leq m \leq 25.4, \text{ and } 1884.3 \text{ MPa} \leq \sigma_u \leq 1943.6 \text{ MPa}.$$

From the results it can be seen that there is a large difference between the layer 4 results and the results from the analysis of the complete set of specimens (layers 1-6). The confidence intervals for  $m$ , however, slightly overlap ([25.0, 77.0] for layer 4 and [15.9, 25.4] for all specimens) which is not the case for  $\sigma_u$  results ([1681.2, 1734.5] for layer 4 and [1884.3, 1943.6] for all specimens).

The distinct difference in the Weibull stress is obvious from the Weibull plot which is shown in Fig. B.7. The seven specimens with the highest  $\sigma_W$ -values are contained in layers 5 and 6. The full ranking scheme is given in Table B.5. The curve for all specimens shows a pronounced kink with these seven values being at the right side of the kink. These values contribute essentially to the lowering of the  $m$  value compared to the layer 4 results.

The pronounced kink of the Weibull plot indicates that  $\sigma_W$  is possibly bi-modally distributed. This, in principle, calls for additional fractographic investigations which have to reveal different fracture mechanisms present in the different layers, thus leading to a different behaviour at low and high  $\sigma_W$ -values, respectively.

From this it can be concluded that the main source of scatter is not generated by varying stress-strain law characteristics. Scatter in the  $\Delta D$  at fracture would still be present, even if the variation of stress-strain law characteristics was accounted for by some scaling procedures.

From Fig. B.7 it is also evident, that there is a tendency for the two parameters  $m$  and  $\sigma_u$  to be statistically dependent, i.e. high  $m$ -values lead to lower  $\sigma_u$ -values.

## Beneficial use of bootstrap simulations

This chapter contains results obtained with the help of some novel statistical techniques, known as bootstrap or resampling techniques. These methods have been well-known since about 20 years in the field of biological and medical research [8] both because of the large economic impact of statistically-based decisions and because of the lack of analytical solutions for sophisticated statistical models, but they are relatively unknown in materials science. The methods rely heavily on the availability of sufficient computing power, which is the main reason for their coming up recently only.

Their essential advantage is that analytical solutions are replaced by suitably designed statistical simulations. Parametric as well as non-parametric stochastic models can be used which makes it possible to adapt modelling to the available knowledge.

### 4.1 Background and procedure

Traditional methods of statistical inference are based on the fact that estimates of parameters calculated from random samples are themselves random variates (also known as statistics). Often, they have known statistical distributions, at least under certain conditions with respect to the sample value distribution and/or the sample size. As an example, the mean of a sample of independent identically distributed variables is known to follow a normal distribution for large sample sizes, the variance of a random sample of known mean value is  $\chi^2$ -distributed. If closed-form distributions cannot be obtained, it is sometimes possible to obtain special-case solutions and to derive general solutions by an appropriate transformation of the variables. This is for instance done in [7] for the distribution of the maximum likelihood estimates  $\hat{m}$  and  $\hat{\sigma}_u$  which can be obtained from the special case of a Weibull distribution with  $m = \sigma_u = 1$ , i.e. a standard exponential distribution.

From the known statistical distributions, confidence intervals are obtained easily by using quantiles of the respective distributions.

In the present case, however, where the Weibull stress  $\sigma_W$  is the random variable under consideration, the situation becomes somewhat difficult. From the definition of  $\sigma_W$  (see Eq. (2.2)), it follows that  $\sigma_W$  itself contains the (originally unknown) distribution parameter  $m$ . This, in principle, violates the conditions of applicability of conventional methods of statistical inference. The results obtained for estimates and confidence intervals are therefore only approximate.

### 4.1.1 Basic idea of bootstrapping

One way of dealing with the lack of closed-form expressions for statistical quantities is to use Monte Carlo methods. Bootstrapping is one of them. In the following, a *very* concise description of the bootstrap method mainly based on [8] is given. (We use the traditional nomenclature, hats ( $\hat{\cdot}$ ) denote estimates, asterisks ( $\cdot^*$ ) denote quantities related to bootstrap samples,  $n$  is the sample size,  $B$  is the number of bootstrap simulations.)

Suppose we observe  $x_1, \dots, x_n$  independent data points, from which we compute a statistic of interest  $s(x_1, \dots, x_n)$ .

A *bootstrap sample*  $x^* = (x_1^*, \dots, x_n^*)$  is obtained by randomly sampling,  $n$  times, with replacement, from the original data points  $x_1, \dots, x_n$ . If this is repeated  $B$  times, we can generate a large number of independent bootstrap samples  $x^{*1}, \dots, x^{*B}$ , each of size  $n$ .

Corresponding to each bootstrap sample  $x^{*b}$  there is a bootstrap replication of  $s$ , namely  $s(x^{*b})$ , the value of the statistic of interest computed for sample  $x^{*b}$ .

Besides  $s(x^{*b})$ , we also obtain a bootstrap estimate for its standard deviation, namely

$$\widehat{\text{se}}_{\text{boot}} = \left\{ \frac{1}{B-1} \sum_{b=1}^B [s(x^{*b}) - s(\cdot)]^2 \right\}^{\frac{1}{2}} \quad (4.1)$$

where  $s(\cdot) = \sum_{b=1}^B s(x^{*b})/B$  is the mean value of the statistic  $s$  after  $B$  bootstrap simulations.

### 4.1.2 Bootstrap confidence intervals

Using  $\widehat{\text{se}}_{\text{boot}}$  and  $s(\cdot)$ , it is possible to attribute confidence intervals to bootstrap estimates  $\hat{\theta}^*(\cdot) = \sum_{b=1}^B \hat{\theta}^*(b)/B$ , where  $\hat{\theta}^*(b) = s(x^{*b})$  is the bootstrap replication of  $\hat{\theta} = s(x_1, \dots, x_n)$  as defined above. For example, we obtain the usual standard normal  $(1 - 2\alpha)$ -confidence interval for  $\theta$ , which is

$$\hat{\theta} \pm z^{(\alpha)} \times \widehat{\text{se}} \quad (4.2)$$

where  $z^{(\alpha)}$  is the  $\alpha$ -quantile of a standard normal distribution, e.g.  $z^{(0.95)} = 1.645$  for the 90% confidence intervals. This leads to the so-called *standard bootstrap confidence intervals* which still rely on normal theory assumptions as can be seen from Eq. (4.2), which only holds exactly if  $\hat{\theta}$  follows a normal distribution.

But it is also possible to obtain accurate confidence intervals for non-normally distributed statistics, i.e. without relying on normal theory assumptions. This is done by using  $\hat{G}$ , the cumulative distribution of the bootstrap replications  $\hat{\theta}^*$ . The  $1 - 2\alpha$  *percentile interval* for  $\theta$  is defined by the  $\alpha$ - and  $(1 - \alpha)$ -quantiles of  $\hat{G}$ . From  $B$  independent bootstrap samples, we obtain the percentile confidence intervals by taking the  $B \times \alpha$ th value in the ordered list of the  $B$  bootstrap replications of  $\hat{\theta}^*$  as the lower limit and the  $B \times (1 - \alpha)$ th value of the list as the upper limit of the confidence interval. These empirical percentiles are denoted  $\hat{\theta}_B^{*(\alpha)}$  and  $\hat{\theta}_B^{*(1-\alpha)}$  respectively and the percentile confidence interval reads

$$[\hat{\theta}_B^{*(\alpha)}, \hat{\theta}_B^{*(1-\alpha)}] \quad (4.3)$$

for a confidence level of  $1 - 2\alpha$ .

Some drawbacks of the percentile intervals with respect to coverage probabilities are handled by an improved version of the percentile method including bias correction in the bootstrap replications. Bias correction  $z_0$  is obtained from the cumulative distribution function  $\hat{G}$  of the bootstrap replication and the original estimate  $\hat{\theta}$  of the original sample via

$$z_0 = \Phi^{-1}(\hat{G}(\hat{\theta})) \quad (4.4)$$

where  $\Phi^{-1}(\cdot)$  is the inverse standard normal cumulative distribution function (CDF). We obtain the bias-corrected bootstrap confidence intervals as

$$\left[ \Phi(2z_0 + \Phi^{-1}(\alpha)), \Phi(2z_0 + \Phi^{-1}(1 - \alpha)) \right] \quad (4.5)$$

with  $z_0$  from Eq. (4.4). Confidence intervals according to Eq. (4.5) are used throughout the presentation of the bootstrap results in the following section. Calculation of  $z_0$  is indicated in some of the Figures, e.g. B.11, B.12, B.13.  $z_0 = 0$  indicates no bias correction. In that case, the lower limits of the confidence intervals would coincide with the empirical CDF shown, as nearly is the case in Figure B.13.  $z_0 \neq 0$  leads to a shift of the confidence intervals.

Further improvements of confidence levels can be obtained by application of still more advanced methods like the  $BC_a$ -method or the ABC-method suggested in the statistical literature. These methods have not yet been implemented and therefore are not used in the sequel.

## 4.2 Results

The general ideas presented in the previous section are now applied to the specific case of the Weibull parameter estimation of the Weibull stress.

### 4.2.1 Weibull stress bootstrapping procedure

In the present case, where we are interested in statistical inference about the distribution parameters  $m$  and  $\sigma_u$  of  $\sigma_W$ , the basic situation is as follows: the original sample consists of the  $n$  values of  $\Delta D$  at fracture or - equivalently - of the  $n$  maximum principal stress envelopes at fracture, from which the  $\sigma_W$ -values are computed. In this case, the statistic under consideration is not available as an analytical expression, but only numerically as a result of an iteration algorithm. When doing bootstrap simulations, this does not cause any problem. The procedure is explained for the parameter  $m$  for the sake of simplicity; more accurately, we should use  $(m, \sigma_u)$  as a two-dimensional statistic.

From the original sample, we obtain the original estimate  $\hat{\theta} = \hat{m}$  using the iterative maximum likelihood procedure together with the usual maximum likelihood confidence intervals.

Bootstrapping is now performed by randomly sampling,  $n$  times, with replacement, from the sample of the  $\Delta D$  at fracture, from which  $n$  values,  $\sigma_{W(1)}^*, \dots, \sigma_{W(n)}^*$ , are computed. This is repeated  $B$  times, thus giving  $B$  samples  $\sigma_W^{*b}$ . For each bootstrap sample, a value of  $\hat{m}^*(b)$  is obtained by the iterative maximum likelihood procedure.

After completion of the bootstrap simulations, the bootstrap confidence intervals are generated according to Eq. (4.5) for confidence levels  $\alpha = 0.02; 0.05; 0.10$  in agreement with the maximum likelihood confidence intervals available from literature [3, 7].

## 4.2.2 Bootstrap results for parameter estimation

The pairs of corresponding outcomes for the parameters of the Weibull stress distribution,  $(\hat{m}^*(b), \hat{\sigma}_u^*(b))$ ,  $b = 1, \dots, B$  are directly available from the bootstrap simulation.  $m$  and  $\sigma_u$  appear to be strongly correlated as can be seen from Figure B.8 for the layer 4 data. There is a large variability in  $\hat{m}^*$  with values as large as  $\approx 400$ , which obviously originates from the quite small sample containing  $\Delta D$ -values that are very close to each other and lead to very high  $m$ -estimates if they dominate a bootstrap sample.

The strong dependency between  $m$  and  $\sigma_u$  is also apparent for the complete set of 32 specimens, as visible in Figure B.9.

An interesting feature can be observed in Fig. B.10. There are two slightly overlapping regions of pairs  $(\hat{m}^*, \hat{\sigma}_u^*)$  corresponding to layer 4 results and to results of the complete set of 32 specimens, indicating that the correlation of both variables is indeed very strong and that small sample results, though fully contained in a larger sample, may have completely different statistical properties. In the present case, bi-modality appears in the complete sample, but not in the small subsample.

Incidentally, this remarkably strong dependency of the two parameters does not occur in the case of a Weibull parameter estimation for strength measurements in ceramics. Even if a strong R-curve behaviour suggests some deviation from the Weibull distribution assumptions, the correlation seems to be very small [12].

## 4.2.3 Bootstrap results for confidence intervals

Figure B.11 shows the bootstrap results for  $m$  in terms of the empirical CDF  $\hat{G}$  for the layer 4 specimens. Bootstrap confidence intervals for confidence levels are indicated by horizontal lines at the appropriate CDF levels of 2, 5, and 10%, respectively, corresponding to 96%-, 90%-, and 80%- confidence intervals. From the value of the bias correction variable  $z_0 = -0.52$ , it can be seen that there is a considerable bias in the bootstrap estimate towards higher values. The confidence interval limits are therefore shifted towards lower  $m$ -values, as can be seen in Figure B.11 (see also Table B.6 for the numerical results). The shape of  $\hat{G}(m)$  indicates that there is a considerable fraction of quite large values of  $m$  in the simulation.

This is not the case if all specimens are considered. Figure B.12 shows the corresponding results. The bias of  $m$  is quite small, as indicated by  $z_0 = -0.11$ . Hence, the confidence limits are quite close to the corresponding CDF values. The results for  $\sigma_u$  are shown in Figure B.13 (numerical results can be found in Table B.7). For  $\sigma_u$ , we notice a slight

bias towards lower values, which has to be taken into account. Results for both layer 4 and the complete set are compared in Figure B.14. There is a pronounced kink in the layer 4 curve, which is not present in the curve for all specimens. For clarity, overlapping confidence intervals are marked with arrows. A comparison with ML confidence intervals is given in Tables B.6 and B.7.

Contrary to the distribution of  $\hat{\sigma}_u$ , which is quite symmetric, there is a pronounced unsymmetry in the distribution of  $\hat{m}$ , with a long tail for large  $m$ -values for both the layer 4 subset and the complete set of specimens.

#### 4.2.4 Bootstrap results for probabilities

Bootstrapping does not only allow conclusions to be drawn with regard to parameters, but also inferences to be made regarding the entire CDF. This is not possible using ML confidence intervals. As an example, layer 4 results of the experimentally obtained sample ( $n=7$ ) Weibull stresses at fracture are shown as an empirical cumulative distribution function, the dashed step curve in Fig. B.15. The dashed smooth curve shows the ordinary ML approximation, while the solid curves are obtained for the confidence limits for the lower regime of the Weibull stress, i.e. the lower and upper limits for  $m$  and  $\sigma_u$ , respectively. The two solid step curves are results of bootstrap simulations. They show 90% confidence intervals for the  $i$ -th value of an ordered sample of Weibull stresses and give some idea about the scatter of the data without using any assumption of distributions.

The same confidence intervals are shown in Fig. B.16 for all specimens, where also the influence of increasing bootstrap sample size is shown. Increasing the bootstrap sample size from  $B = 200$  to  $B = 1000$  does not have any significant influence on the width of the confidence intervals. This confirms that bootstrap simulations usually tend to give stable results with a quite small number of simulations.

In Figure B.17, bootstrap confidence limits of the empirical CDF both for layer 4 and for all specimens are plotted. It can be seen that, except in the very low tail of the curves, the 90% confidence bands of the empirical CDF do not overlap, which indicates that both samples are not statistically compatible.

This is a consequence of our attempt to fit a unimodal CDF to a bi-modal distribution. Additionally, we must take into account that  $m$  itself influences the  $\sigma_W$ -value. A smaller  $m$ -value will tend to shift the  $\sigma_W$ -sample towards higher values, whereas for larger values of  $m$  there will be a tendency for  $\sigma_W$  in the opposite direction, giving smaller Weibull stresses.



## Summary and conclusions

As part of an ESIS Round Robin activity coordinated by GKSS, Geesthacht, the Weibull stress parameters of a ferritic steel with the German designation of 22 NiMoCr 3 7 have been determined using the ESIS P6 procedure.

The overall goal of the Round Robin was to assess uncertainties in the identification of cleavage fracture parameters from numerical analysis of notched tensile specimen cleavage fracture data due to numerical differences and due to different procedures in the statistical inference methods used for parameter evaluation.

In the contribution presented in this paper, the main effort was put on a comprehensive stochastic analysis of the data using standard and advanced stochastic methods, while continuum mechanics models were taken from standard FE material libraries.

The evaluation was divided into two steps, as suggested by the task description (Appendix C) due to some scatter in the stress-strain behaviour of the material, possibly caused by local variations of the material which was taken from different places of a forged ring segment.

In a first step, specimens from a prescribed subset (layer 4) were selected for evaluation. Due to the fact that the sample size was seven specimens only, the statistical evaluation will contribute mostly to a numerical comparison of the results between the participants of the Round Robin.

In a second step, the complete set of 32 specimens were analysed, which allowed to perform a statistical analysis. Results of the Weibull stress at fracture show that there may be a change in the fracture behaviour between lower and higher  $\sigma_W$ -values leading to a bimodal distribution of  $\sigma_W$ . The reason for this, e.g. different fracture mechanisms, has to be confirmed by additional fractographic investigations.

The numerical procedure for the determination of the parameters of  $\sigma_W$  did not cause any difficulties. Convergence was very fast, even in the case of the small sample size.

A third step was additionally performed. Originally, it was not intended to be part of the Round Robin activity. Within this step, an attempt was made to apply advanced stochastic methods for the calculation of distributions and confidence intervals for the statistical parameters of  $\sigma_W$ . These so-called bootstrap or resampling methods do not necessarily rely on specific distribution assumptions, but use the empirical distribution of the sample for the determination of the relevant quantities by statistical simulation. A strong correlation between  $m$  and  $\sigma_u$  was found as a result of the simulation.

From the simulation, it was also possible to obtain the statistical distribution of the bootstrap estimates of  $m$  and  $\sigma_u$ , which allowed the determination of confidence intervals for  $m$  and  $\sigma_u$ .

Moreover, confidence limits for the entire distribution function of  $\sigma_w$  could be obtained by this method with quite moderate bootstrap sample sizes. With respect to computing time, this is an important aspect because of the iterative procedure used to calculate  $\sigma_w$  which calls for efficient numerical procedures.

A comparison of the bootstrap results with the ML results (Tables B.6 and B.7) is made on the basis of the 90% confidence intervals (i.e. the 0.05- and 0.95-quantiles). The results show that for the layer 4 results the BC 90% interval for  $m$  is much more narrow than its ML counterpart, especially on the right side, towards larger  $m$ -values. The lower limits of the  $\sigma_u$ -confidence intervals nearly coincide for both methods, the upper BC limits, if available, are considerably larger than the corresponding ML limits. This is mainly due to the large bias correction  $z_0 = 0.482$  in this case and leads to a BC interval length which is almost twice that of the ML counterpart.

For the complete set, the BC 90% interval for  $m$  is not so much different from its ML counterpart, but shifted to the right and gives somewhat higher values for both left and right confidence limits. The  $\sigma_u$ -confidence intervals in this case are considerably wider compared to those based on the ML estimates. The width of the  $\sigma_u$  interval is an indication of the correlation of  $m$  and  $\sigma_u$ , due to the fact that an increase in  $m$  leads to decreasing values of  $\sigma_u$ .

Finally, it should be noted that an evaluation of the cleavage fracture data consists of (at least) two parts which should be equally emphasized. One part is the numerical evaluation of the cleavage fracture parameters using appropriate continuum mechanics and stochastic tools and models. The other, at least as important, part is the fractographic investigation of the fractured specimens. Interpretation of the numerical results is incomplete without fractography. Conversely, results of the numerical analysis indicate possible topics of fractographic investigations.

# References

- [1] H. Riesch-Oppermann, A. Brückner-Foit, WEISTRABA - A code for the numerical analysis of Weibull stress parameters from ABAQUS finite element stress analyses - Procedural background and code description -, FZKA Report 6155, Forschungszentrum Karlsruhe, 1998.
- [2] W. Brocks, Numerical Round Robin on Micromechanical Models, IWM-Bericht T 8/95, Fraunhofer-IWM, Freiburg, 1995.
- [3] ESIS P6 - 98, Procedure to Measure and Calculate Local Approach Criteria Using Notched Tensile Specimens, ESIS Document, March 1998.
- [4] ABAQUS/Standard User's Manual (Version 5.4), Hibbit, Karlsson & Sorensen, Inc. 1994.
- [5] E.J. Gumbel, Statistics of Extremes, Columbia University Press, 1958.
- [6] B.F. Kimball, On the choice of plotting positions on probability paper, J. of the Amer. Statist. Assoc. **55** (1960), 546-560.
- [7] D.R. Thoman, L.J. Bain, C.E. Antle, Inferences on the Parameters of the Weibull Distribution, Technometrics, **11** (1969), 445-460.
- [8] B. Efron, R.J. Tibshirani, An introduction to the bootstrap, Chapman & Hall, Boca Raton, 1993.
- [9] T.J. DiCiccio, B. Efron, Bootstrap confidence intervals, Statistical Science **11** (1996), 189-211.
- [10] E. Fuller, Mechanical properties of brittle materials, National Institute of Standards and Technology (NIST), MSEL Annual Report 1997 (unpublished).
- [11] J. Cuccio et al., Probabilistic Methods for Ceramic Component Design and Implications for Standards, in: C.R. Brinkman, S.F. Duffy (eds.): Life Prediction Methodologies and Data for Ceramic Materials, ASTM STP 1201, ASTM, Philadelphia, 1994.
- [12] H. Riesch-Oppermann, (unpublished results).



# Appendix A

## Scheme of the iterative maximum likelihood procedure

The determination of the two parameters  $m$  and  $\sigma_u$  was performed iteratively according to the following scheme, since  $\sigma_W$  depends on the (unknown) parameter  $m$ .

Step 1: A starting value of e.g.  $m = 20$  is used and the Weibull stress  $\sigma_W$  at fracture is calculated for each fractured specimen (i.e. at different load steps according to the experimental loading parameter) as described above.

Step 2: A plot file is generated containing the results in increasing order of Weibull stress  $\sigma_W$  together with  $\ln \ln[1/(1 - \overline{F(\sigma_{W(i)})})]$  as a function of  $\ln \sigma_{W(i)}$ , where  $\sigma_{W(i)}$  is the Weibull stress of the specimen with rank  $i$  and  $\overline{F(\sigma_{W(i)})} = i/(N + 1)$  is the mean (cumulative) frequency of the  $i$ -th observation (use of  $i/(N + 1)$  as plotting position is generally recommended for statistical reasons – e.g. [5] –, although it does not play any role provided that the maximum likelihood method is used for parameter estimation). As the theoretical relation between failure probability and  $\sigma_W$  is given by

$$P_f = 1 - \exp \left[ - \left( \frac{\sigma_W}{\sigma_u} \right)^m \right] ,$$

a plot of  $\ln \ln[1/(1 - \overline{F(\sigma_{W(i)})})]$  versus  $\ln \sigma_{W(i)}$ , where  $\sigma_{W(i)}$  is the “experimental” Weibull stress for the specimen with rank  $i$ , should give an approximately linear relation.

(Step 2 is only for illustrative purposes and, thus, not necessary for Step 3)

Step 3: The maximum likelihood method is used to determine the parameters  $m$  and  $\sigma_u$  of the Weibull distribution of the Weibull stress. The maximum likelihood estimators of  $m$  and  $\sigma_u$  are denoted by  $\hat{m}$  and  $\hat{\sigma}_u$ , respectively.  $\hat{m}$  is the solution of the non-linear equation

$$\frac{N}{\hat{m}} + \sum_{i=1}^N \ln \sigma_{W(i)} - N \frac{\sum_{i=1}^N \sigma_{W(i)}^{\hat{m}} \ln \sigma_{W(i)}}{\sum_{i=1}^N \sigma_{W(i)}^{\hat{m}}} = 0$$

which is obtained by e.g. an interval sectioning procedure. Using  $\hat{m}$ , the maximum likelihood estimator  $\hat{\sigma}_u$  is obtained from the equation

$$\hat{\sigma}_u = \left( \frac{1}{N} \sum_{i=1}^N \sigma_{W(i)}^{\hat{m}} \right)^{\frac{1}{\hat{m}}}$$

The parameter  $\hat{m}$  is corrected with the unbiasing factor  $b(N)$  according to  $\hat{m}_{unb} = \hat{m} * b(N)$ .

Step 4: If the maximum likelihood estimators  $\hat{\sigma}_u$  and  $\hat{m}_{unb}$  agree within a fixed tolerance with those of the previous iteration, their values are considered acceptable. Otherwise, steps 2-4 are repeated. A flow diagram is given in Figure A.1 to illustrate the iterative procedure.

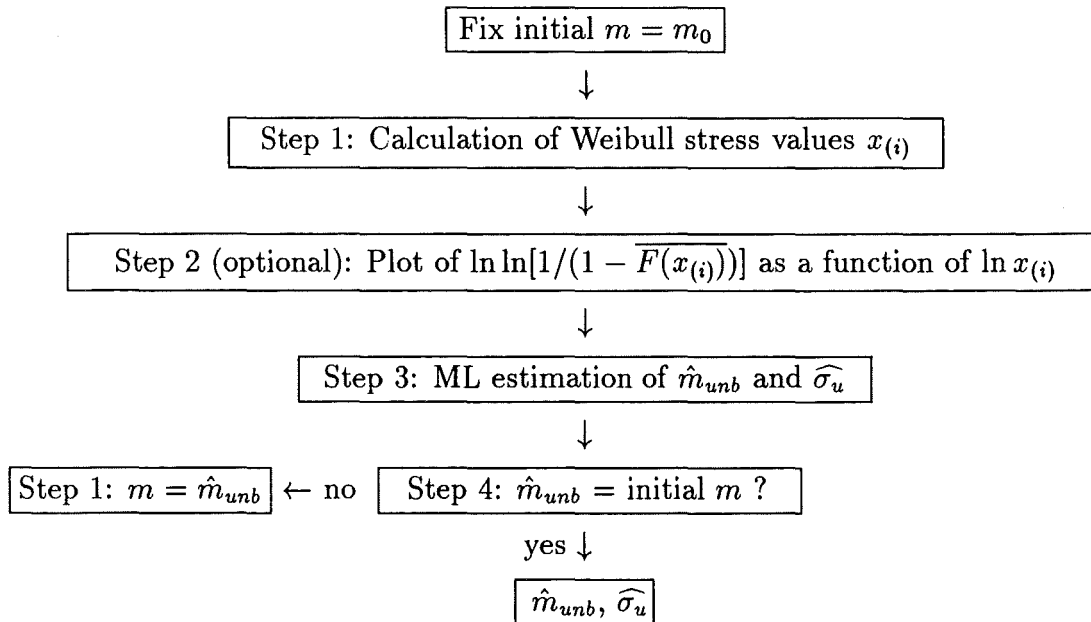


Figure A.1: Flow diagram for the iterative Weibull parameter estimation procedure

# Appendix B

## Figures and Tables

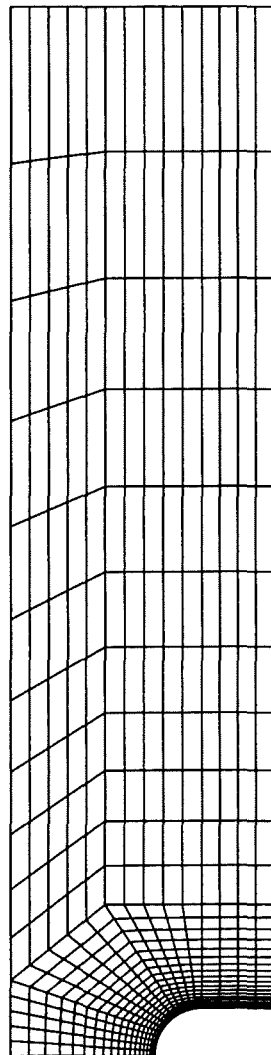


Figure B.1: Meshing of the specimen

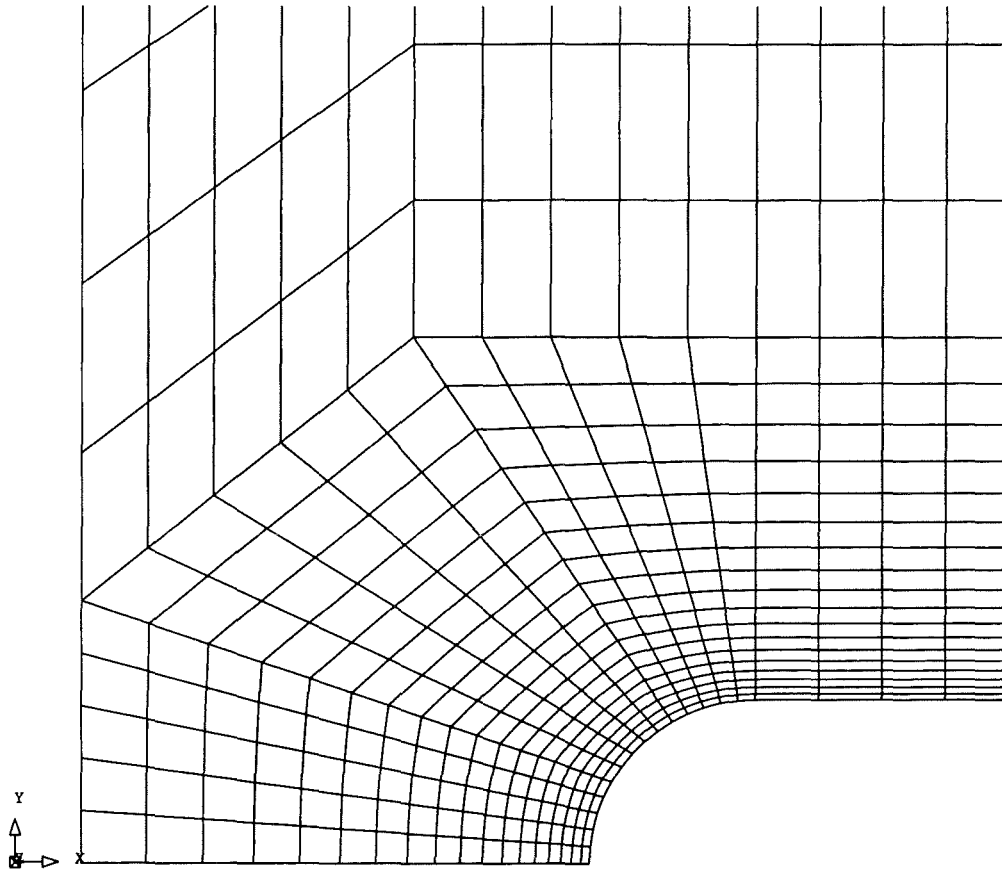


Figure B.2: Detail of specimen meshing at the notch root

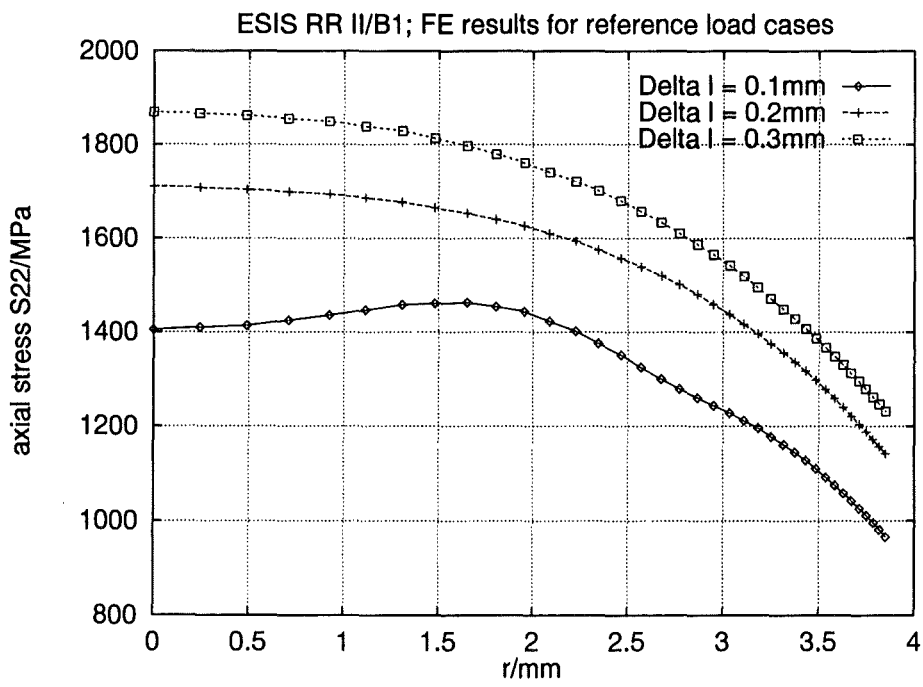


Figure B.3: Axial stress distribution along  $z = 0$

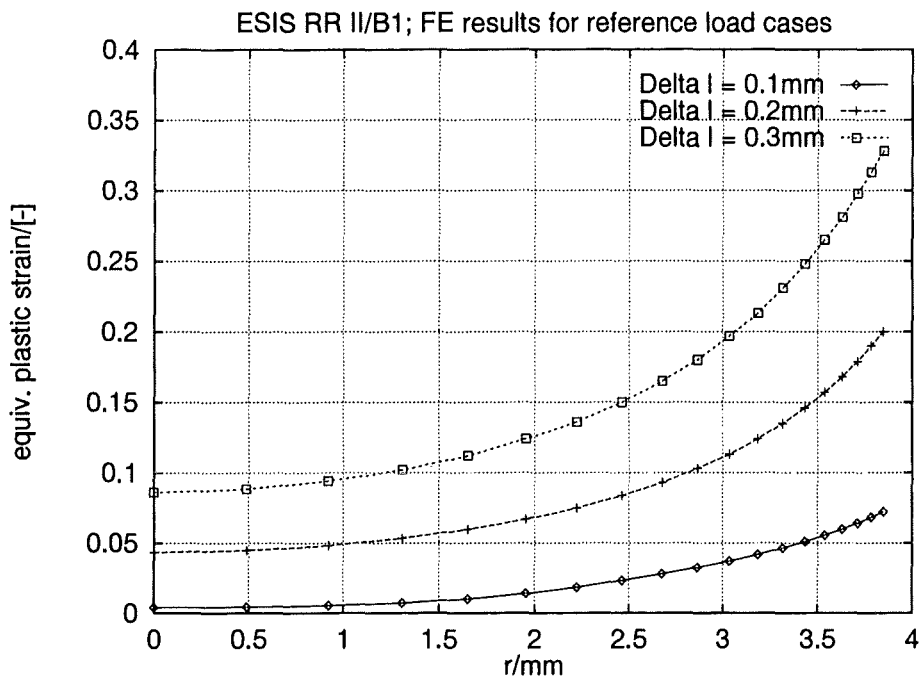


Figure B.4: Distribution of equivalent plastic strain along  $z = 0$

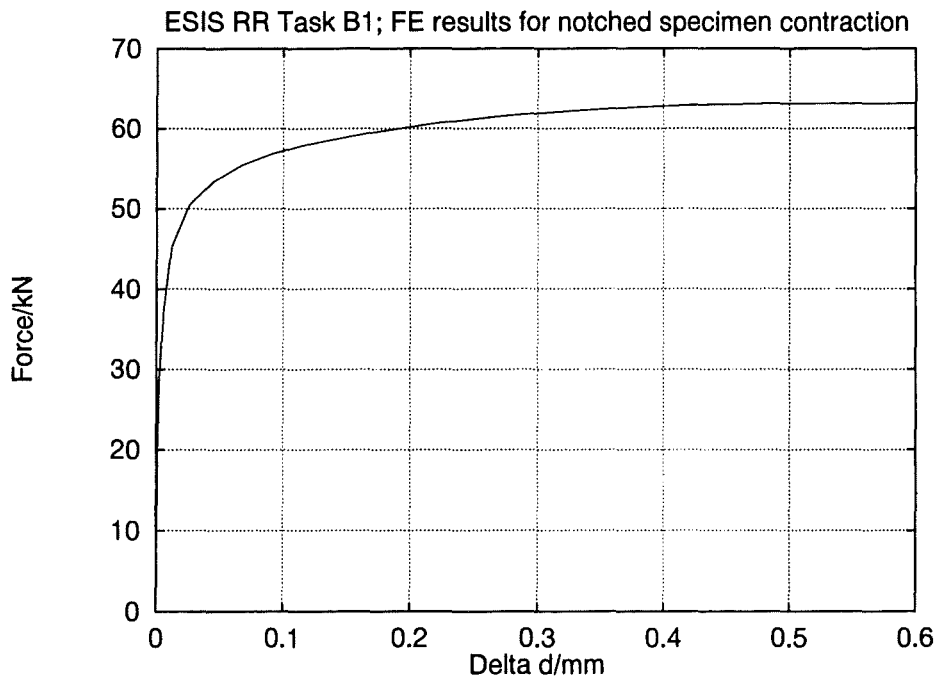


Figure B.5: Simulation of notched specimen contraction

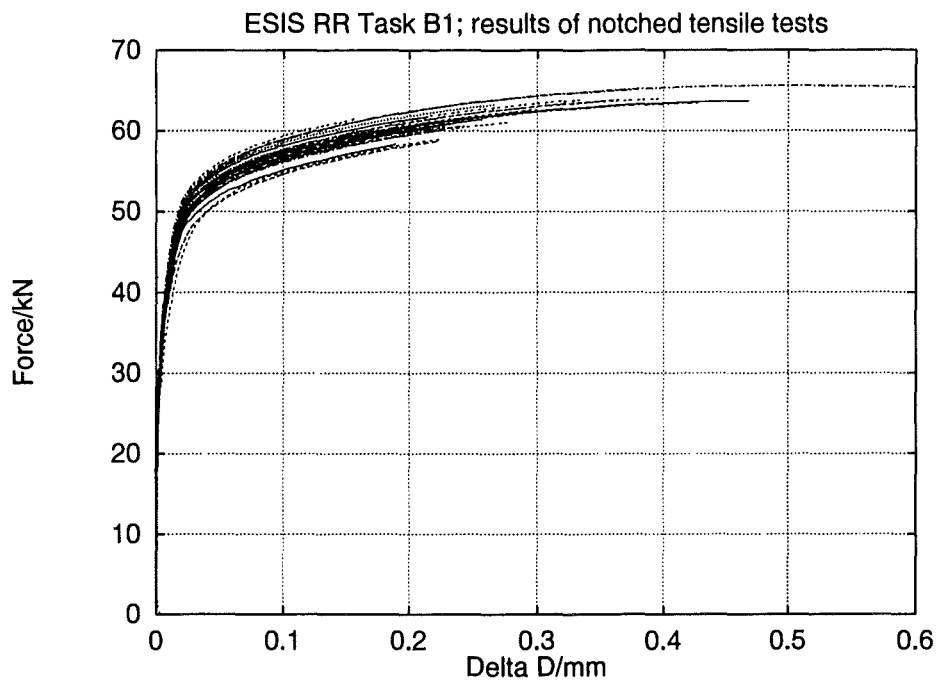


Figure B.6:  $F - \Delta D$  records of all tested specimens in the ESIS Round Robin

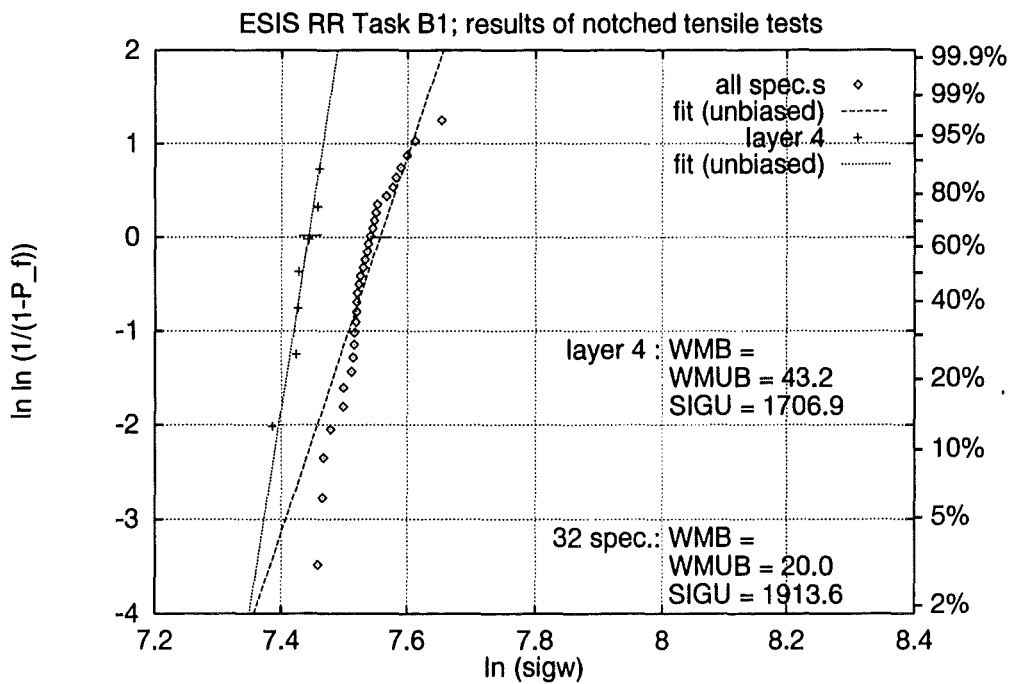


Figure B.7: Weibull stress results for all specimens compared to results for layer 4

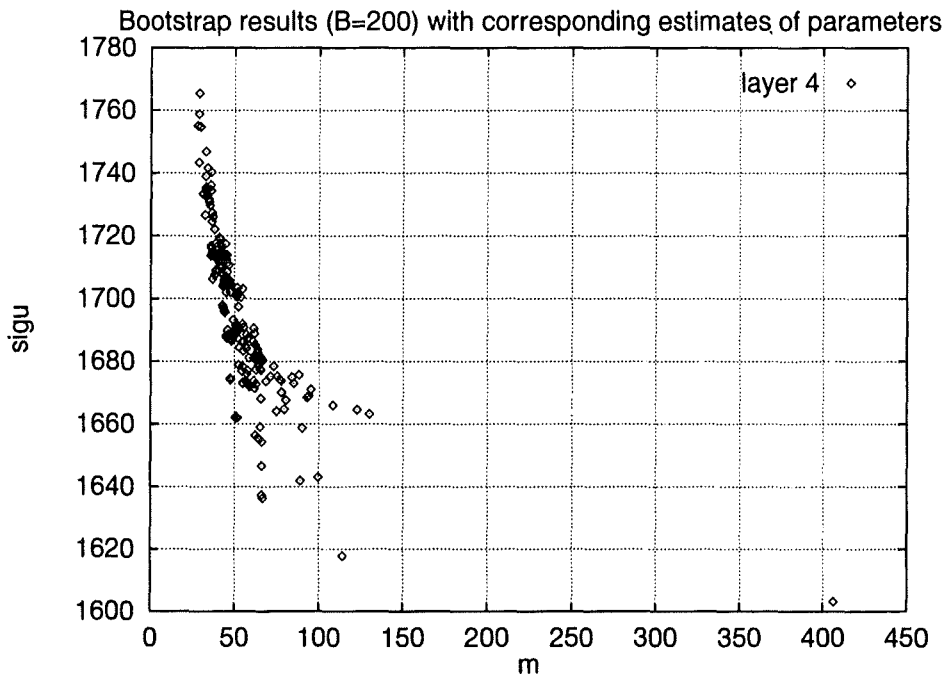


Figure B.8: Bootstrap results for layer 4

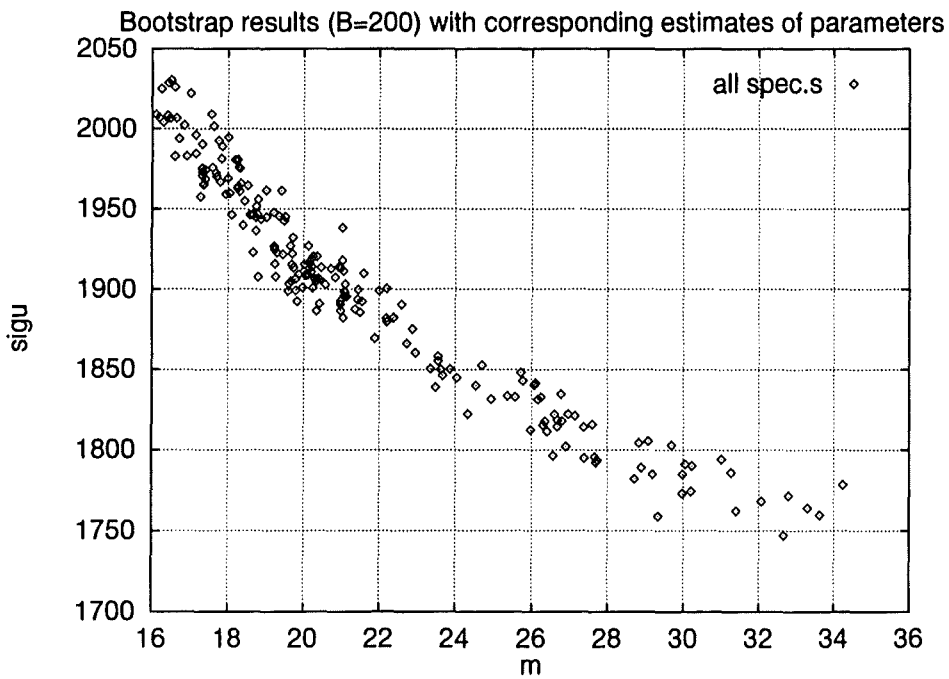


Figure B.9: Bootstrap results for all specimens

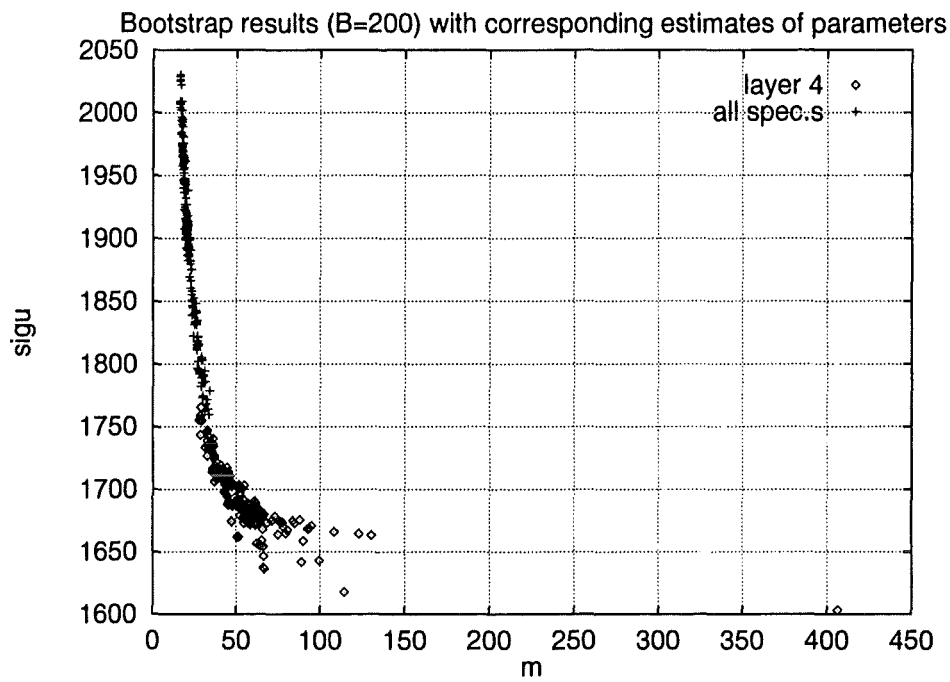


Figure B.10: Bootstrap results for layer 4 and all specimens compared

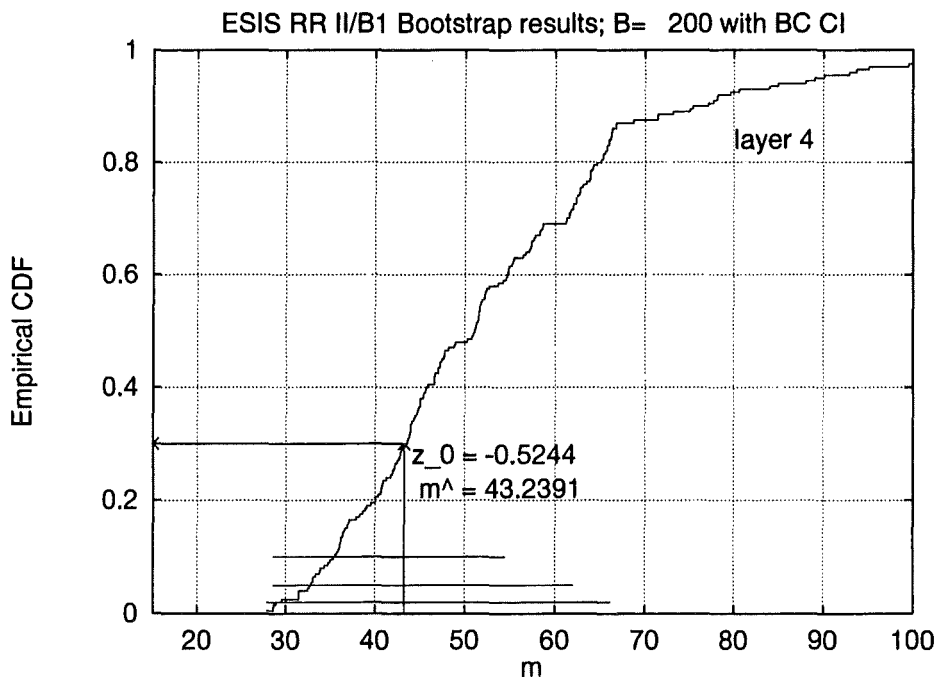


Figure B.11: Bootstrap confidence intervals of  $m$  for layer 4

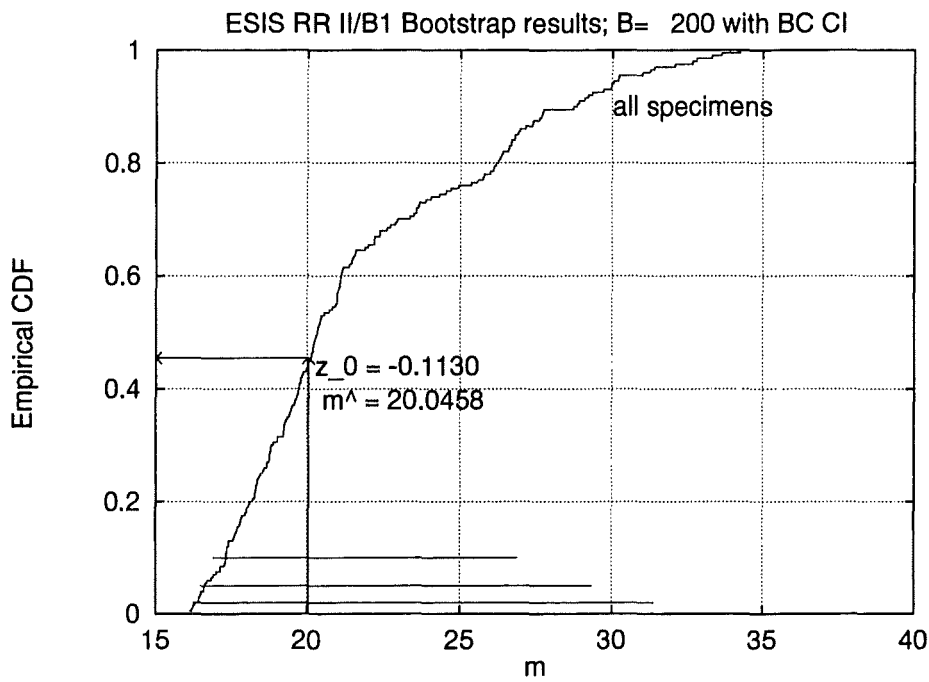


Figure B.12: Bootstrap confidence intervals of  $m$  for all specimens

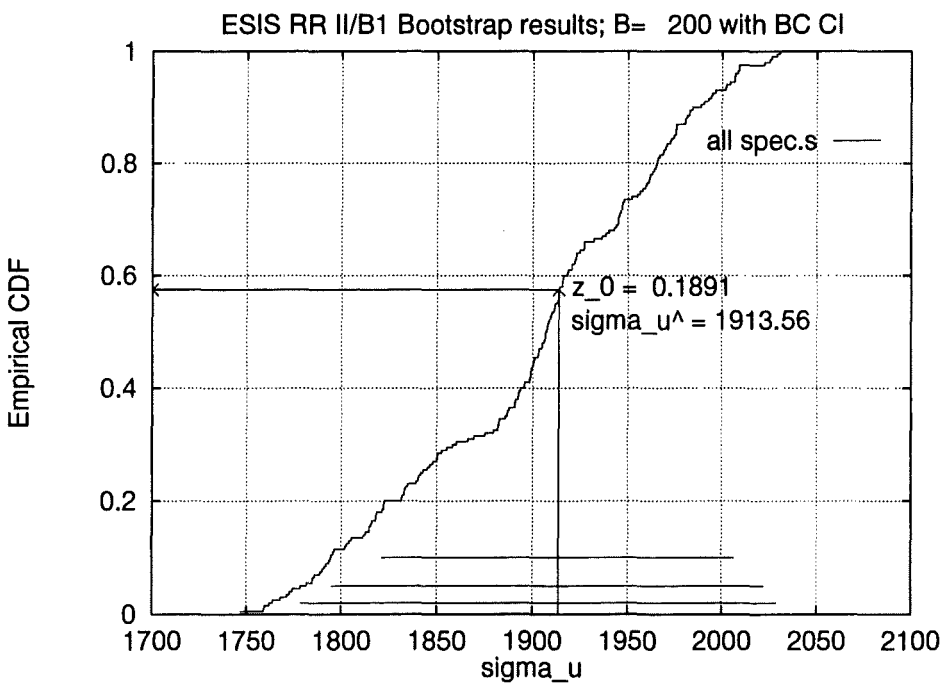


Figure B.13: Bootstrap confidence intervals of  $\sigma_u$  for all specimens

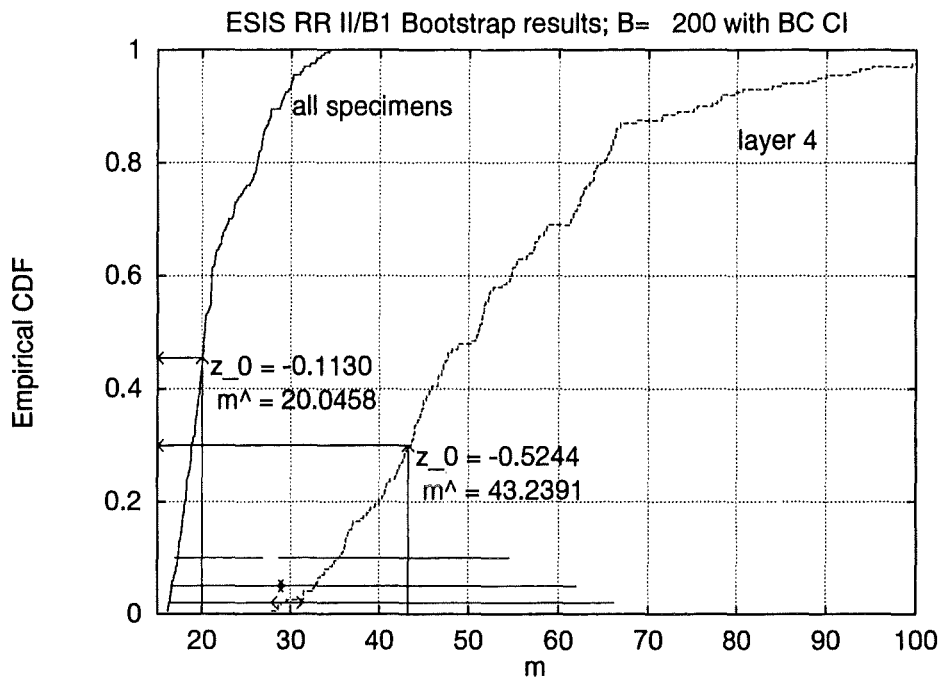


Figure B.14: Bootstrap confidence intervals of  $m$  for layer 4 and all specimens compared

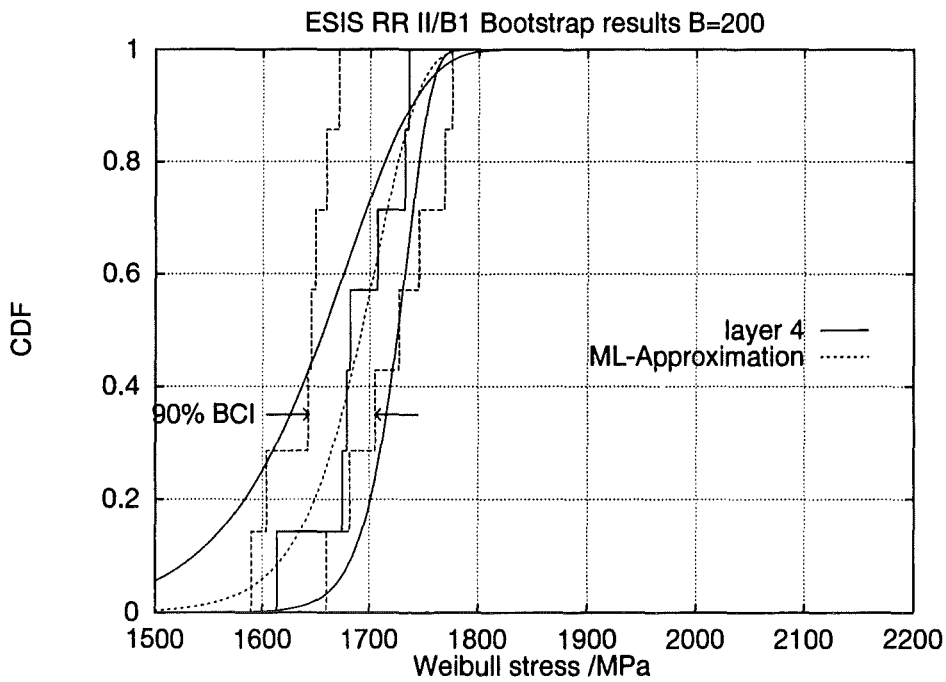


Figure B.15: Bootstrap confidence intervals (BCI) of empirical CDF for 'layer 4' specimens (dashed step curves) compared with lower ML confidence curves (solid continuous curves)

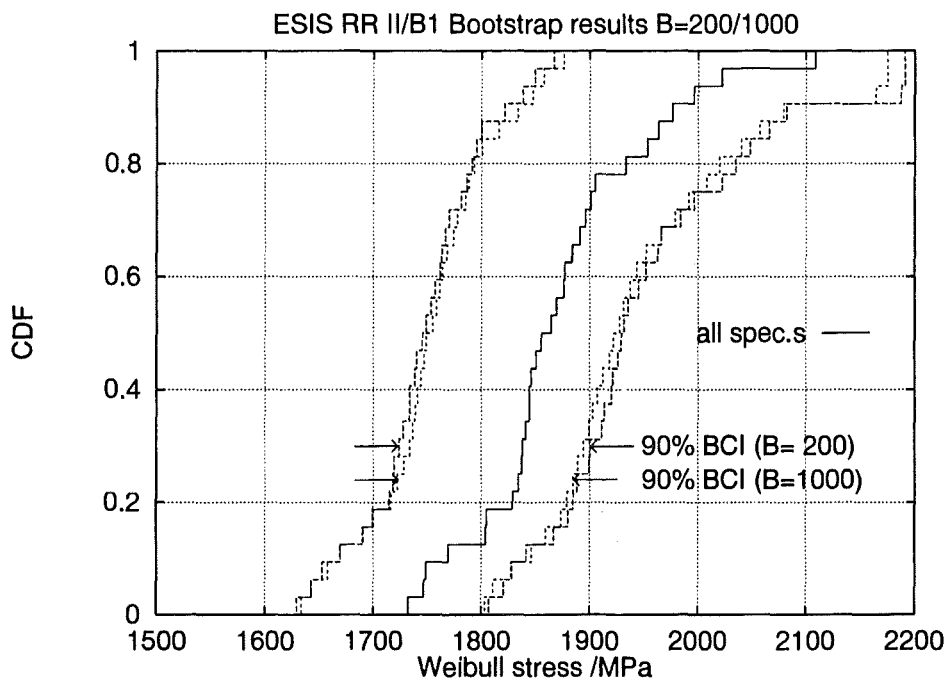


Figure B.16: Bootstrap confidence intervals of empirical CDF for all specimens; influence of bootstrap size

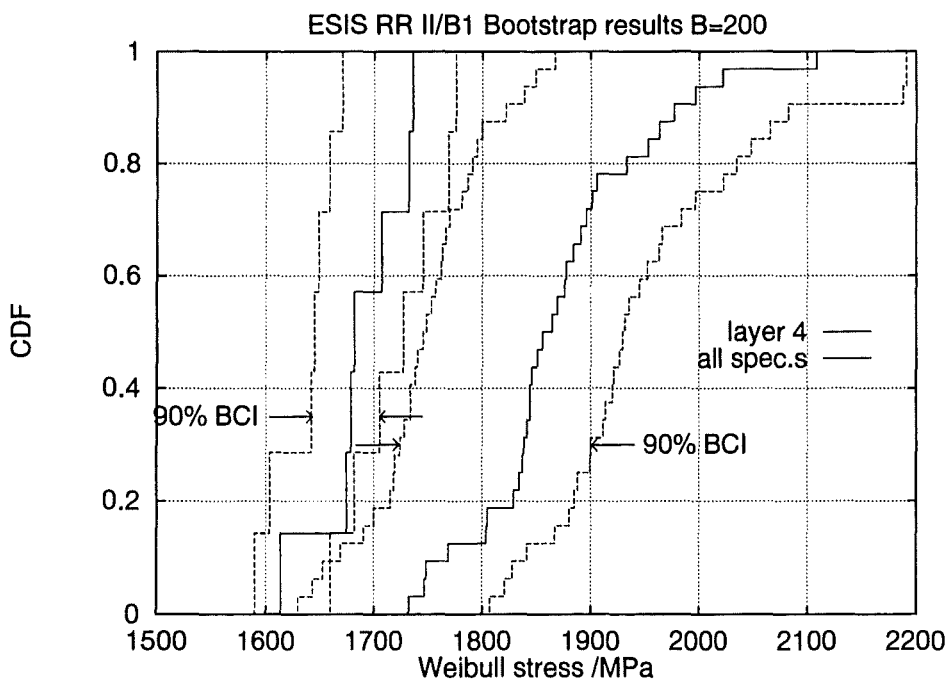


Figure B.17: Bootstrap confidence intervals (BCI) of empirical CDF for 'layer 4' (left) and all specimens (right) compared

$\Delta l/\text{mm}$	$-\Delta d/\text{mm}$	F/kN
.00	.00000	.00
.01	.00044	9.45
.02	.00090	18.93
.03	.00202	28.17
.04	.00525	37.10
.05	.01158	45.26
.06	.02544	50.49
.07	.04471	53.42
.08	.06645	55.42
.09	.09004	56.80
.10	.11476	57.88
.12	.16675	59.42
.14	.21960	60.65
.16	.27280	61.58
.18	.32560	62.19
.20	.37860	62.65
.22	.43180	62.96
.24	.48540	63.11
.26	.53920	63.11
.28	.59380	63.11
.30	.64880	62.96
.32	.70460	62.65
.34	.76140	62.34
.36	.81880	62.04
.38	.87720	61.73
.40	.93640	61.27

Table B.1: Force and diameter contraction of FE calculation at prescribed imposed displacements  $\Delta l$  at  $u_z = 28$  mm (reference steps "1", "2", and "3" are indicated)

step designation	prescribed displacement $u_z$ [mm]	in the centre element; averaged over Gauss points		in the notch root element; averaged over Gauss points	
		$\epsilon_p$ [-]	$\sigma_I$ MPa	$\epsilon_p$ [-]	$\sigma_I$ MPa
"1"	0.1	.004388	1410.	.06985	979.
"2"	0.2	.04355	1700.	.1935	1152.5
"3"	0.3	.08578	1855.	.3195	1240.
"Df4"	.1194	.01108	1541.02	.09388	1026.12
"Df16"	.1366	.0177	1626.21	.1153	1058.25
"Df10"	.1379	.0182	1632.62	.1168	1060.39
"Df25"	.1389	.0186	1635.95	.1180	1062.05
"Df31"	.1501	.02325	1668.27	.1318	1081.43
"Df28"	.1671	.03038	1681.16	.1530	1110.40
"Df34"	.1694	.03128	1683.26	.1560	1113.42

Table B.2: Local quantities in the centre and notch root element, respectively, for layer 4 specimens.

step designation	prescribed displacement $u_z$ [mm]	reduction of diameter $\Delta D$ [mm]	Force [kN]	$m = 22$		$m = 43.2$	
				$\sigma_w$ [MPa]	$P_f(\sigma_w)$ [%]	$\sigma_w$ [MPa]	$P_f(\sigma_w)$ [%]
"1"	0.1	.11476	57.88	—	—	—	—
"2"	0.2	.37860	62.65	—	—	—	—
"3"	0.3	.64880	62.96	—	—	—	—
"Pf10% $m_{22}$ "				1661.0	10	—	—
"Pf10%"				—	—	1620.3	10
"Df4"	.1194	0.1672	59.36	1743.8	26.5	1613.5	8.40
"Df16"	.1366	0.2124	60.45	1804.0	47.70	1674.6	35.45
"Df10"	.1379	0.2158	60.51	1808.0	49.37	1678.6	38.45
"Df25"	.1389	0.2184	60.57	1810.9	50.59	1681.6	40.80
"Df31"	.1501	0.2484	61.11	1837.5	62.15	1707.0	63.30
"Df28"	.1671	0.2928	61.81	1868.3	75.36	1732.3	84.95
"Df34"	.1694	0.2986	61.90	1872.6	77.08	1736.0	87.46

Table B.3: Global quantities for layer 4 specimens.

step designation	prescribed displacement $u_z$ [mm]	reduction of diameter [mm]	Force [kN]	$m = 22$		$m = 20.0$	
				$\sigma_w$ [MPa]	$P_f(\sigma_w)$ [%]	$\sigma_w$ [MPa]	$P_f(\sigma_w)$ [%]
"1"	0.1	.11476	57.88	—	—	—	—
"2"	0.2	.37860	62.65	—	—	—	—
"3"	0.3	.64880	62.96	—	—	—	—
"Pf10% $m_{22}$ "				1681.27	10	—	—
"Pf10%"				—	—	1710.36	10
1	.1122	.15002	58.77	1702.3	12.63	1732.5	12.75
2	.1149	.15675	58.99	1716.7	14.77	1747.0	14.88
3	.1152	.15750	59.00	1718.3	15.03	1748.6	15.14
4	.1194	.16813	59.36	1738.8	18.65	1769.2	18.74
5	.1279	.19010	59.92	1773.6	26.42	1804.0	26.42
6	.1281	.19062	59.94	1774.4	26.62	1804.8	26.62
7	.1350	.20860	60.37	1798.3	33.28	1828.9	33.21
8	.1366	.21280	60.45	1803.4	34.82	1834.0	34.73
9	.1376	.21540	60.51	1806.4	35.77	1837.0	35.68
10	.1379	.21620	60.53	1807.3	36.06	1837.9	35.96
11	.1389	.21880	60.57	1810.3	37.01	1840.9	36.90
12	.1399	.22140	60.64	1813.2	37.95	1843.9	37.83
13	.1399	.22140	60.64	1813.2	37.95	1843.9	37.83
14	.1405	.22300	60.67	1814.9	38.51	1845.6	38.39
15	.1423	.22760	60.76	1819.8	40.15	1850.6	40.02
16	.1441	.23240	60.85	1824.4	41.71	1855.2	41.57
17	.1479	.24220	61.04	1833.2	44.80	1864.1	44.66
18	.1501	.24800	61.13	1838.1	46.56	1869.1	46.42
19	.1533	.25660	61.27	1844.7	49.01	1875.9	48.89
20	.1538	.25780	61.30	1845.8	49.40	1876.9	49.28
21	.1573	.26700	61.45	1852.4	51.90	1883.8	51.81
22	.1611	.27700	61.61	1859.0	54.43	1890.6	54.39
23	.1641	.28500	61.71	1864.2	56.42	1895.9	56.42
24	.1671	.29280	61.82	1869.1	58.36	1901.1	58.40
25	.1694	.29880	61.90	1873.1	59.91	1905.2	59.98
26	.1839	.33700	62.34	1900.3	70.44	1932.9	70.57
27	.1943	.36440	62.58	1920.0	77.64	1952.9	77.77
28	.1998	.37900	62.68	1930.0	81.04	1963.1	81.17
29	.2070	.39800	62.81	1942.9	85.04	1976.2	85.15
30	.2182	.42780	62.95	1962.8	90.25	1996.3	90.33
31	.2332	.46780	63.07	1988.1	95.06	2021.9	95.10
32	.2858	.61000	63.01	2074.4	99.91	2108.8	99.91

Table B.4: Global quantities (all spec's).

specimen rank	1	2	3	4	5	6	7	8	9	10	11	12	13	14	15	16
layer No.	2	6	2	4	1	1	2	4	5	4	4	2	1	3	3	3
specimen rank	17	18	19	20	21	22	23	24	25	26	27	28	29	30	31	32
layer No.	1	4	6	5	5	5	6	4	4	5	6	6	6	5	6	6

Table B.5: Ranking of specimens and corresponding layers

Quantiles	ML intervals		BC intervals	
	$m$	$\sigma_u$	$m$	$\sigma_u$
0.02	20.7	1672.2	27.8	1669.0
0.05	25.0	1681.2	28.6	1675.3
0.10	29.3	1688.3	28.6	1683.3
0.90	69.5	1727.4	54.5	1755.1
0.95	77.0	1734.5	62.0	1765.4
0.98	85.4	1744.7	66.2	-

Table B.6: Maximum likelihood (ML) confidence intervals of layer 4 results compared with bias-corrected (BC) bootstrap confidence intervals

Quantiles	ML intervals		BC intervals	
	$m$	$\sigma_u$	$m$	$\sigma_u$
0.02	16.8	1891.1	16.2	1778.6
0.05	15.9	1884.3	16.5	1794.9
0.10	14.9	1875.5	16.9	1821.2
0.90	24.2	1936.9	26.9	2006.7
0.95	25.4	1943.6	29.3	2022.1
0.98	26.7	1951.2	31.4	2028.7

Table B.7: Maximum likelihood (ML) confidence intervals of all specimens compared with bias-corrected (BC) bootstrap confidence intervals



# Appendix C

## Task Description

The description of the ESIS Round Robin Phase II Task B1 as issued by GKSS, Geesthacht, is enclosed in Appendix C.

to all participants of the

**ESIS TC 8 Numerical Round Robin  
on Micro-Mechanical Models Phase II**

Ihr Zeichen/Ihre Nachricht

Unser Zeichen

Durchwahl/Telefon:

Durchwahl Telefax:

Datum

**G. Bernauer**

04152/87- 2618

04152/87- 2625

**February 11, 1999**

### **Round Robin on Micro-Mechanical Models, Phase II, Task B1**

Dear participant,

please find enclosed the detailed description of Task B1 of the round robin on micro-mechanical models, Phase II. You will also receive an e-mail with the experimental load vs. reduction of diameter data or – attached to this letter – a diskette containing the data. Please let us know if you do not receive any e-mail or disk.

We wish you good success and interesting results.

We intend to write a report and present the activities and the first results of Task A1 and A2 at the ESIS TC 8 meeting in Swansea at 15th of April.

Yours sincerely,



(Dr.-Ing. G. Bernauer)



(Prof. Dr.-Ing. W. Brocks)

Enclosure

Mitglied der Hermann von Helmholtz-Gemeinschaft Deutscher Forschungszentren

European Structural Integrity Society (ESIS)  
Technical Committee 8: Numerical Methods

Numerical Round Robin on Micro-Mechanical Models

Phase II

Task B1

G. Bernauer, W. Brocks

February, 1999

# Contents

## 1. Subject

## 2. Notched round tensile bar tests

2.1. Specimens of layer "4"

2.2. All specimens

## 3. Task

3.1. Analysis of the specimens of layer "4" (obligatory)

3.1.1. Meshing and FE formulation

3.1.2. Material properties

3.1.3. Calculation of fracture probabilities and determination of WEIBULL parameters

3.2. Analysis of the entire set of specimens (voluntary)

## 4. Reporting of the results

## 5. Contact address and deadline

## 6. References

### **Appendix: Equations and parameters of the BEREMIN model for the analysis of cleavage fracture**

## 1. Subject

The tasks A1 and A2 of Phase II of the ESIS TC8 numerical round robin on micro-mechanical models were distributed in September 1997 and March 1998, respectively. This document now represents the continuation of the round robin which covers Task B1:

Numerical analysis of notched tensile specimens in order to identify critical parameters for cleavage at low temperatures.

- The first part of task B1 is obligatory. It is concerned with the application of the BEREMIN model to a subset of specimens which have been taken out of a limited region of the material block and which show a nearly identical load deformation behaviour up to the respective failure point.
- In a voluntary second part, the complete set of all performed tests will be utilised. It is left to the participant to make use of these experimental results with regard to a meaningful statistical characterisation of the conditions for cleavage fracture.

The model which shall be applied is the local approach to cleavage fracture of BEREMIN. In addition, also another statistical model can be taken.

The objective of Task B1 is to determine the model parameters. At the end of the work the results of all participants will be compared in order to get information about the dependencies of the parameters on the finite element programmes and parameter evaluation programmes applied.

In a further step, Task B2, it will be investigated whether it is possible to predict realistic failure probabilities of a C(T) specimen if the critical cleavage parameters determined here are used.

## 2. Notched round tensile bar tests

The basis for the investigations are notched round tensile bars tested at a temperature of  $T = 150^{\circ}\text{C}$ . The specimens were machined from a forged ring segment. A sketch of the position of the specimens is given in Fig. 1. The dimensions of the specimens are outlined in Fig. 2.

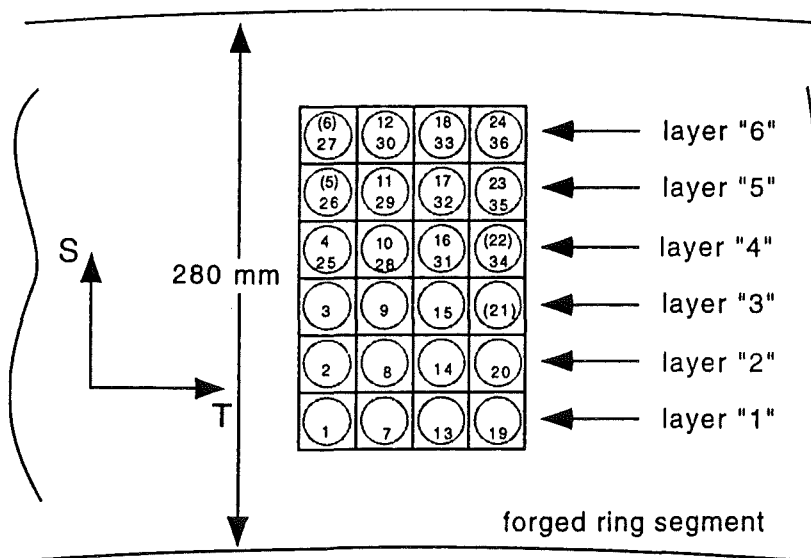


Fig. 1: Plan of specimen locations. Specimens with numbers in brackets have not been tested.

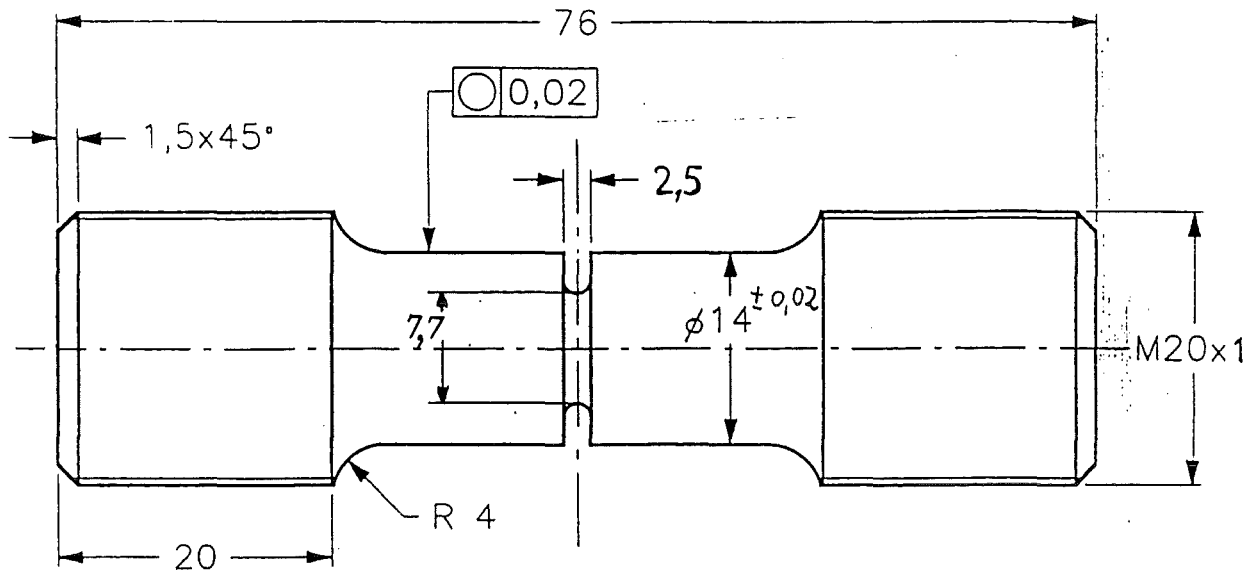


Fig. 2: Test specimen: notched round tensile bar.

The specimens were subjected to a quasi-static displacement controlled loading in axial direction at  $-150^{\circ}\text{C}$ . The loading rate was  $0.2\text{ mm/min}$ . All specimens failed by instable fracture, and the fracture surfaces show pure cleavage facets.

The load vs. reduction of diameter curves of the specimens (Fig. 3 and 4) up to the point of fracture are at the participants' disposal.  $\Delta D$  was measured in the notch root area.

The data of the curves will be sent in ASCII format to the participants either by e-mail or on a 3.5" diskette.

The tests of the notched tensile specimens have shown a correlation between the load displacement behaviour and the position of the specimens in the material block. It could be shown that small variations in the geometry alone cannot be responsible for the differences in the displacement behaviour. That means that not all specimens have the same material properties. Whether the dependence of the material properties on the position concerns only the flow curve or also the WEIBULL parameters is an open problem. The analyses within the present round robin might contribute to a solution of this problem.

Section 2.1. shows the test results of the specimens which have been taken from layer "4" of the block (Fig. 1). They show nearly the same load deformation path. Section 2.2. presents the results of all specimens tested.

## 2.1. Specimens of layer "4"

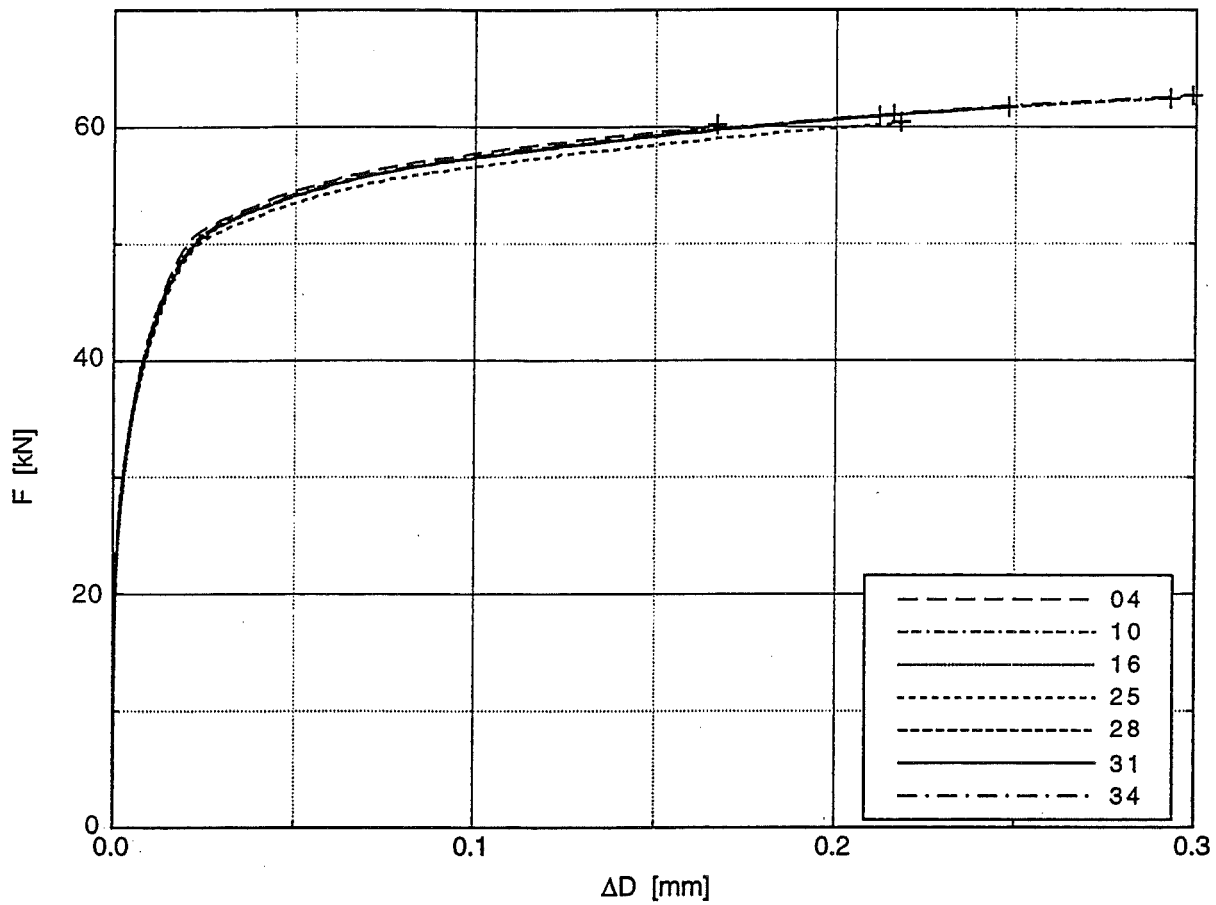


Fig. 3: Load,  $F$ , vs. reduction of diameter,  $\Delta D$ , of the notched tensile specimens of layer "4" up to their respective fracture.

specimen no.	$F$ [kN]	$\Delta D$ [mm]
4	60.18	0.167
16	60.94	0.212
10	61.08	0.216
25	60.42	0.218
31	61.70	0.248
28	62.42	0.293
34	62.69	0.299

Tab. 1: Load,  $F$ , and reduction of diameter,  $\Delta D$ , of the notched tensile specimens at the onset of cleavage fracture.

## 2.2. All specimens

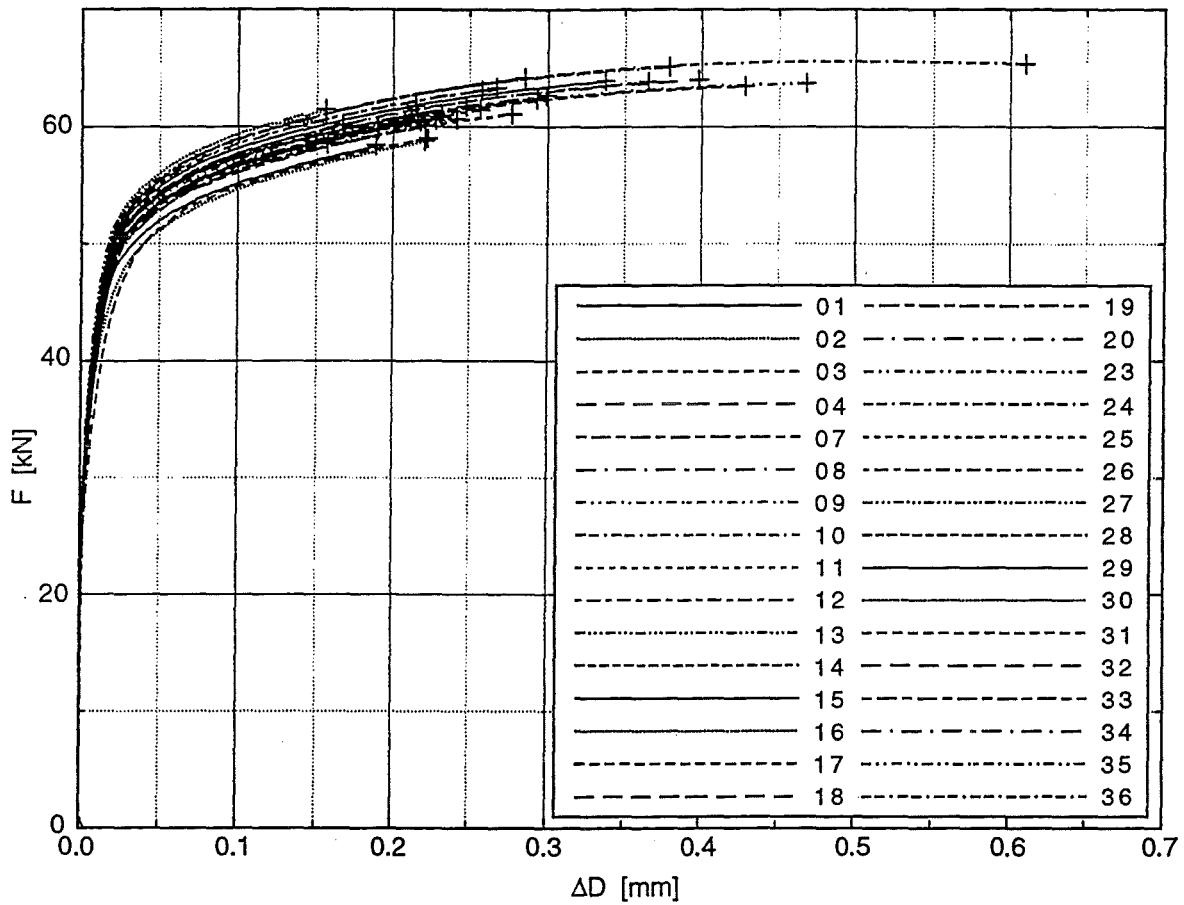


Fig. 4: Load,  $F$ , vs. reduction of diameter,  $\Delta D$ , of all notched tensile specimens up to their respective fracture.

specimen no.	$F$ [kN]	$\Delta D$ [mm]
14	58.69	0.149
30	61.47	0.156
20	58.52	0.157
4	60.18	0.167
1	58.42	0.189
19	59.77	0.190
8	60.50	0.208
16	60.94	0.212
32	61.79	0.215
10	61.08	0.216
25	60.42	0.218
2	58.79	0.221
7	60.06	0.221
3	59.00	0.223
9	60.59	0.228
15	60.88	0.232
13	60.66	0.242

31	61.70	0.248
12	61.46	0.257
35	63.09	0.258
26	63.31	0.267
11	61.06	0.277
33	64.17	0.285
28	62.42	0.293
34	62.69	0.299
29	63.92	0.337
24	63.85	0.365
27	65.12	0.379
18	64.00	0.398
17	63.45	0.428
23	63.69	0.468
36	65.36	0.610

*Tab. 2: Load,  $F$ , and reduction of diameter,  $\Delta D$ , of all notched tensile specimens at the onset of cleavage fracture.*

### **3. Task**

#### **3.1. Analysis of the specimens of layer "4" (obligatory)**

##### **3.1.1. Meshing and FE formulation**

Since geometry and loading are axisymmetric and symmetric to the line bisecting the length, only an axisymmetric quarter section has to be modelled (Fig. 5). The co-ordinate system as shown in the figure together with the following notations shall be used:

- index "r" or "1" for the radial direction,
- index "z" or "3" for the axial direction.

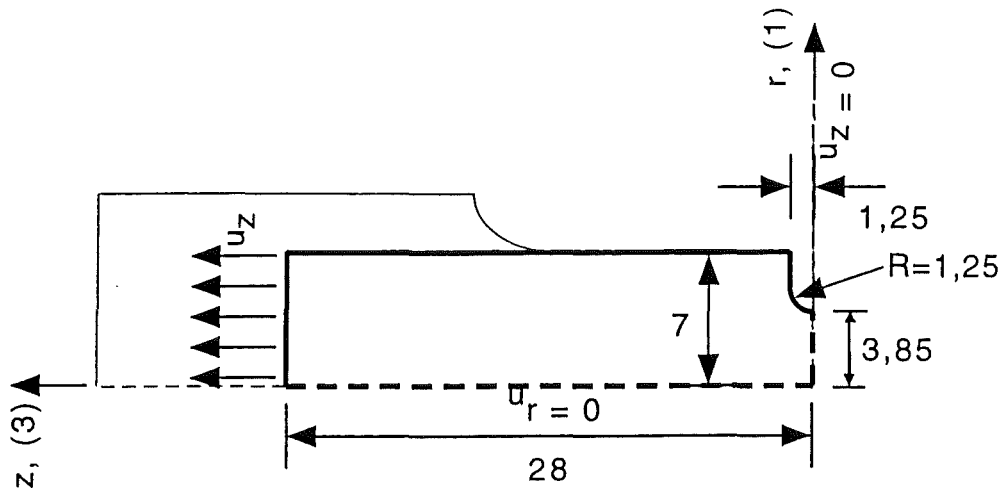


Fig. 5: Axisymmetric quarter section of the specimen, co-ordinate system and boundary conditions. The thin lines outline the specimen, the thick lines show the part of the specimen which is relevant to be modelled. All dimensions in mm.

Meshing is free. Nevertheless, you should keep to the ESIS P6 98 guideline [1] or the following recommendations. An example of a mesh is shown in Fig. 6. Isoparametric quadratic (8 node) elements with reduced integration are recommended. At the notch root an element size between  $0.1 \times 0.1 \text{ mm}^2$  and  $0.15 \times 0.15 \text{ mm}^2$  and at least 8 elements in the fracture plane at  $z = 0$  should be used. This size relates to  $V_o$  (eq. (A2) in the Appendix) which will be set to be  $V_o = (0.1)^3 \text{ mm}^3$  and which is of the same order as the dimensions of microstructural features like ferrite grains. If other than the recommended elements are used, element sizes and integration should guarantee a similar accuracy and resolution. Please, report and explain all deviations from the recommendations.

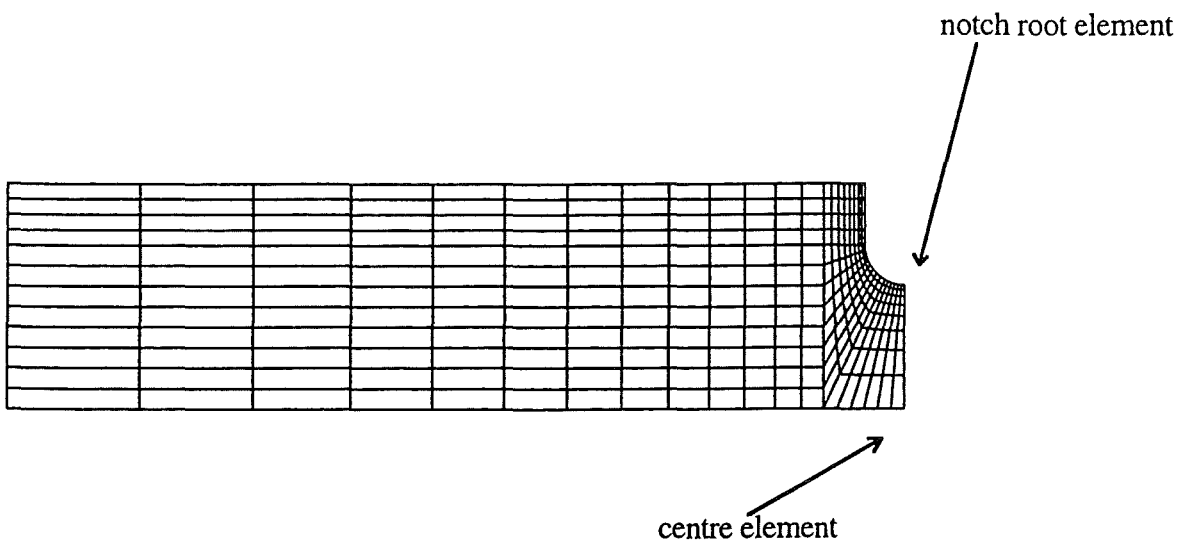


Fig. 6: Example of a FE mesh for the notched tensile specimen.

Boundary conditions, i.e. zero normal displacements, have to be imposed at the two symmetry lines; displacements in length direction at the centre line and in radial direction at the bisection line, respectively, are free. Referring to Fig. 5, the boundary conditions are

$$u_z = 0 \quad \text{if } z = 0 ,$$

$$u_r = 0 \quad \text{if } r = 0 .$$

Loading is applied as homogeneous prescribed displacements  $u_z = f(t)$  in axial direction at the left edge of the model (Fig. 5). All nodes on this line undergo the same displacement. The simulation should be driven that far that all the test are covered, i.e.  $\Delta D = 0.299$  mm for the tests of Tab. 1, or  $\Delta D = 0.61$  mm for the tests of Tab. 2. The time function and the time steps are defined by each participant. However, for the sake of comparison the individually chosen load history has to include the steps which are described in the following table:

step designation	at which the ...
"1"	...prescribed (imposed) displ. is $u_z = 0.1$ mm
"2"	...prescribed (imposed) displ. is $u_z = 0.2$ mm
"3"	...prescribed (imposed) displ. is $u_z = 0.3$ mm

*Tab. 3: Definition of prescribed steps in order to enable comparisons.*

These steps have to be identified by the numbers given in the table. The displacements  $u_z$  are those of one half of the specimen.

The total external force,  $F$ , results from the summation of all nodal forces at the right edge (Fig. 5), multiplied by  $2\pi$  if the unit thickness of the FE model is 1 rad.

A large strain analysis should be preferred. Details of the formulation as, e.g., updated Lagrange-Jaumann, used in the FE code shall be reported together with the results.

### 3.1.2. Material properties

Young's modulus at  $-150^\circ\text{C}$  is  $E = 213\ 000$  MPa and Poisson's ratio  $\nu = 0.3$ .

A true stress vs. true (total) strain curve of the steel at  $-150^\circ\text{C}$  is presented in Fig. 7. With this curve the author of this task was able to simulate the notched tensile specimens quite well. It results from a test of a smooth tensile specimen.

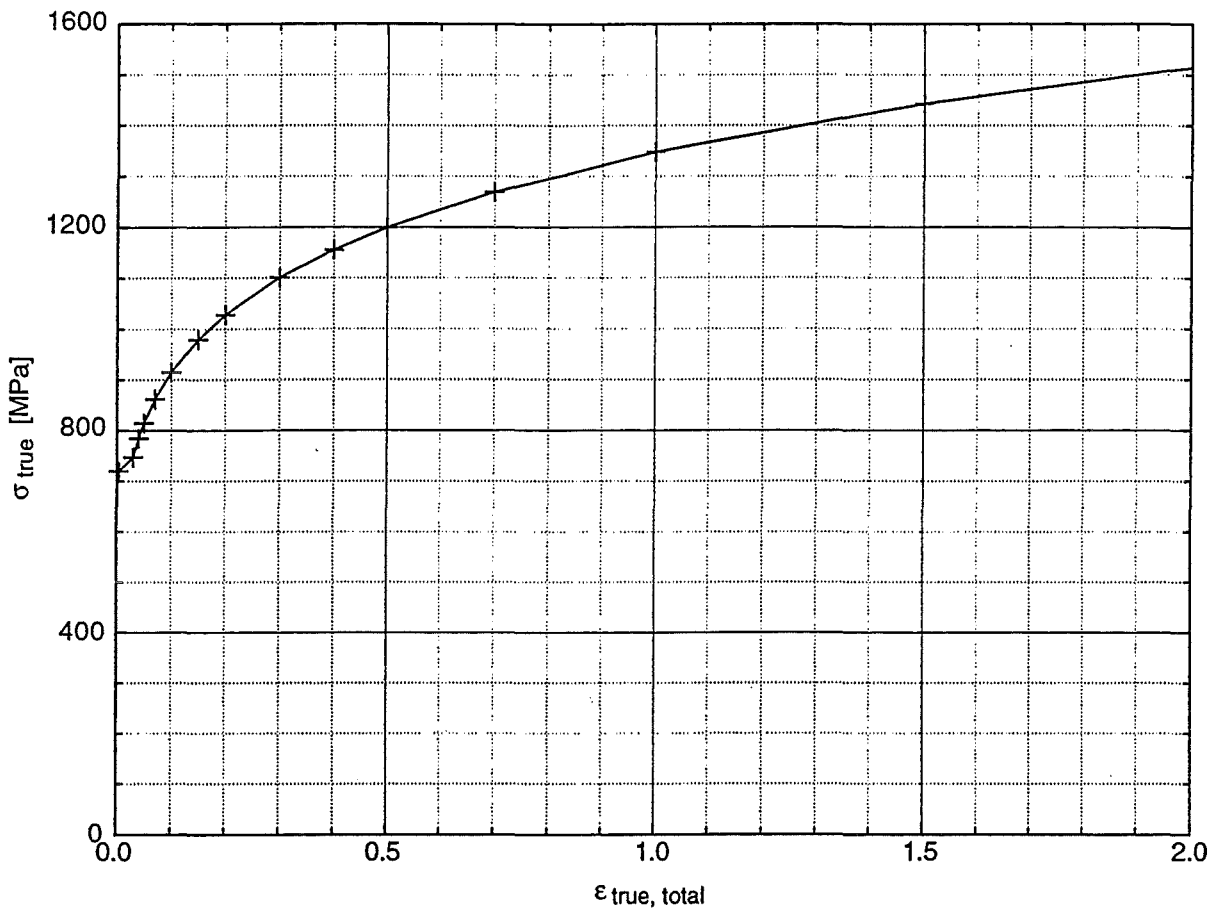


Fig. 7: True stress vs. true (total) strain curve for the simulation of the specimens of layer "4".

The digitised data are given in the following table and will be sent in ASCII format to the participants either by e-mail or on a 3.5" diskette:

true stress $\sigma$ [MPa]	true (total) strain $\varepsilon$
$R_{eL} = 720.0$	$R_{eL}/E = 0.00338028$
747.0	0.03
784.0	0.04
814.0	0.05
861.4	0.07
914.7	0.10
979.3	0.15
1027.9	0.20
1100.4	0.30
1155.0	0.40
1199.2	0.50
1269.0	0.70
1347.5	1.00
1442.6	1.50
1514.2	2.00

Tab. 4: Data points which define the true stress true strain curve. Beyond  $\varepsilon = 0.03$  the curve can be calculated by  $\ln(\sigma / \text{MPa}) = 0.16824 \ln \varepsilon + 7.206$ .

The definitions of stresses and strains refer to an updated Lagrangian formulation. If, due to a different large strain formulation, other definitions of stresses and strains are used, the participant has to make the necessary conversions and to document this in his/her report.

### 3.1.3. Calculation of fracture probabilities and determination of WEIBULL parameters

For the following steps the same procedure as in the preceding round robins [2, 3] can be applied. For details, see the ESIS procedure [1] and the Appendix.

A conventional elastic-plastic analysis based on the theory of von MISES, PRANDTL and REUSS is recommended. According to the BEREMIN model [4, 5], the probability of failure is described by means of WEIBULL statistics. The main outcome of this numerical simulation is the WEIBULL stress,  $\sigma_w$ , which is a value computed on the whole specimen for a given WEIBULL modulus,  $m$ , as a function of a monotonically increasing ranking parameter. Here, the change of diameter,  $\Delta D$ , should be taken for this purpose and for ranking the fractured specimens according to eq. (A3). As described in the Appendix, the WEIBULL stress,  $\sigma_w$ , has to be calculated with  $m = 22$  for the seven time steps, (“Df.” in Tab. 5), which belong to the experimental cleavage fracture events.  $\sigma_w$  is usually calculated by interpolation between neighbouring time steps of the FE analysis. The reference volume is prescribed to be  $V_0 = 0.001 \text{ mm}^3$  for the present calculations. This value relates to microstructural dimensions as well as to the element size of the FE mesh. When performing the summation over the plastically deformed part of the volume of the specimen, be aware that the FE model is axisymmetric, has unit thickness and is symmetric to the centre plane. Hence, if thickness is 1 rad the volume factor equals  $4\pi$ .

Assume that the  $N = 7$  values of  $\sigma_w$  follow a WEIBULL distribution (eq. (A1)) and calculate  $\sigma_u$  with

$$\sigma_u = \sqrt[m]{\frac{1}{N} \sum_{j=1}^N (\sigma_w^{(j)})^m} \quad (1)$$

where  $m = 22$ . Now, calculate the value of  $\sigma_w$  which corresponds to a failure probability of 10 % (eq. (A1)) and give approximate values for the respective load and diameter reduction of the specimen (Tab. 7 in section 4, line “Pf10% $m$ 22”).

step designation	at which the ...
"1"	...prescribed (imposed) displ. is $u_r = 0.1$ mm
"2"	...prescribed (imposed) displ. is $u_r = 0.2$ mm
"3"	...prescribed (imposed) displ. is $u_r = 0.3$ mm
"Df4"	...reduction of diameter, $\Delta D = 2 u_r$ , meets the experimental fracture value of specimen no. 4, $2u_r = 0.167$ mm
"Df16"	...reduction of diameter, $\Delta D = 2 u_r$ , meets the experimental fracture value of specimen no. 16, $2u_r = 0.212$ mm
"Df10"	...reduction of diameter, $\Delta D = 2 u_r$ , meets the experimental fracture value of specimen no. 10, $2u_r = 0.216$ mm
"Df25"	...reduction of diameter, $\Delta D = 2 u_r$ , meets the experimental fracture value of specimen no. 25, $2u_r = 0.218$ mm
"Df31"	...reduction of diameter, $\Delta D = 2 u_r$ , meets the experimental fracture value of specimen no. 31, $2u_r = 0.248$ mm
"Df28"	...reduction of diameter, $\Delta D = 2 u_r$ , meets the experimental fracture value of specimen no. 28, $2u_r = 0.293$ mm
"Df34"	...reduction of diameter, $\Delta D = 2 u_r$ , meets the experimental fracture value of specimen no. 34, $2u_r = 0.299$ mm

Tab. 5: Time steps for calculation of local and global quantities.

Additionally to this task, the WEIBULL parameters,  $\sigma_u V_0^{1/m}$  and  $m$ , shall be determined from the test results of the notched specimens. The parameters can be assessed by the maximum likelihood method [6]. The procedure should follow the ESIS procedure [1]. The basic equations of the procedure are given in the Appendix. Seven tests do, of course, not allow for a satisfactory statistical evaluation, but seem to be sufficient to compare the FE analyses and the evaluation procedures.

Again, calculate  $\sigma_w$  and give values for the load and reduction of diameter for a failure probability of 10 % (Tab. 7 in section 4, line "Pf10%").

A bias correction of the WEIBULL modulus,  $m$ , shall be applied.

Only a limited number of specimens was tested in order to characterise the material. Therefore, the true, unknown WEIBULL parameters of the material cannot be determined exactly. Only intervals can be given, which cover the true parameters with a certain probability. For both WEIBULL parameters, these confidence intervals shall be given, for which the probability is 90 % that the true unknown parameters lie within these intervals. That means that the confidence level for the intervals is 90 % (see eq. (A5) and (A6)).

### 3.2. Analysis of the entire set of specimens (voluntary)

For an application of the BEREMIN model, the stress distributions of all specimens at the moment of cleavage fracture initiation have to be available. A view on Fig. 4 indicates that a single FE simulation will evaluate the stresses of the specimens very insufficiently, because they are

determined by non-uniform flow curves. On the other hand, it is circumstantial to model every specimen with a respective FE calculation. However, the information that specimens show also varying deformation behaviour must not get lost.

The objective of this part of the round robin is to find and to apply a method to use the BEREMIN model in cases, where both, the load deformation paths due to a varying flow behaviour and the onset of cleavage fracture are subject to scatter.

Two ideas for a strategy are suggested:

- Suppose that  $\sigma_w$  is mainly determined by the load,  $F$ . Therefore,  $F$  could be taken as ranking parameter, neglecting that the condition for its monotonic increase for any specimen may not be fulfilled. As the material of the specimen, which shows the highest fracture load, is characterised by a stress strain curve which is different from that given in Tab. 4, you may now scale the stress strain curve of Tab. 4 in an appropriate way, so that the test with the highest fracture load can be modelled. For this purpose it might be useful to keep the hardening exponent, which is defined by  $(d \ln \sigma / d \ln \epsilon)$ , and which is used in the subtitle of Tab. 4, and vary the yield point alone. Now assign the stresses which you have calculated with this simulation to the respective fracture loads of the specimens - the usual application of the BEREMIN model with  $F$  as parameter for ranking the fractured specimens according eq. (A3).
- The following, alternative proposal may lead to comparable results. Suppose that the different load deformation curves are caused by different stress strain curves which can be converted to each other by simple scaling, e.g. changing the yield point and keeping the hardening exponent. As a consequence, the effect of scaling the stress strain curves used in the FE calculation could also be achieved by taking the FE simulation of section 3.1. and multiplying the stresses with different factors which can be read from the ratio of the specimens load level and the load level of the simulation.

Please, report on your method, the idea and the assumptions you have made. Determine the WEIBULL parameters and calculate the respective 90 % confidence intervals.

#### 4. Reporting of the results

Each participant shall report the following details and results:

1. plot of the FE mesh of the specimen and dimensions of the notch root elements;
2. information about the FE code and the algorithms used, especially if self developed codes or user supplied routines have been applied;
3. description of the equations and procedures if other cleavage fracture models or procedures than that described in the appendix are applied;
4. information, whether or not the stresses are averaged within the elements before they are put to the power  $m$  (see the Appendix);

5. graph of load vs. reduction of diameter (twice  $u_r$ ); send an ASCII data table of the data points, which describe the curve, via e-mail or 3<sup>1</sup>/<sub>2</sub>" diskette.
6. send an ASCII data table of local quantities either via e-mail or 3<sup>1</sup>/<sub>2</sub>" diskette, including the following lines (see section 3.1. for the definition of the step designations):

step designation	prescribed displacement $u_z$ [mm]	in the centre element, averaged over the Gauss points		in the notch root element, averaged over the Gauss points	
		$\epsilon_p$ [-]	$\sigma_I$ [MPa]	$\epsilon_p$ [-]	$\sigma_I$ [MPa]
"1"	0.1				
"2"	0.2				
"3"	0.3				
"Df4"					
"Df16"					
"Df10"					
"Df25"					
"Df31"					
"Df28"					
"Df34"					

Tab. 6: Results of Task B1: Local quantities in the centre element and in the notch root element, averaged over the Gauss points: accumulated plastic strain,  $\epsilon_p$ , and first principle stress,  $\sigma_I$ .

7. result of determination of  $\sigma_u$  with given  $m = 22$ ,  $V_0 = 0.001 \text{ mm}^3$ :

$\sigma_u = \underline{\hspace{2cm}}$  MPa

bias correction ( $N = 7$ ):

$m_{cor} = \underline{\hspace{2cm}}$

90 % confidence intervals ( $N = 7$ ,  $\alpha = 0.1$ ):

$\underline{\hspace{2cm}} \leq m \leq \underline{\hspace{2cm}}$ ,  $\underline{\hspace{2cm}} \text{ MPa} \leq \sigma_u \leq \underline{\hspace{2cm}} \text{ MPa}$

8. result of WEIBULL parameter estimation procedure ( $V_0 = 0.001 \text{ mm}^3$ ):

$m = \underline{\hspace{2cm}}$ ,  $\sigma_u = \underline{\hspace{2cm}}$  MPa

bias correction ( $N = 7$ ):

$m_{cor} = \underline{\hspace{2cm}}$

90 % confidence intervals ( $N = 7$ ,  $\alpha = 0.1$ ):

$\underline{\hspace{2cm}} \leq m \leq \underline{\hspace{2cm}}$ ,  $\underline{\hspace{2cm}} \text{ MPa} \leq \sigma_u \leq \underline{\hspace{2cm}} \text{ MPa}$

9. send an ASCII data table of global quantities either via e-mail or 3<sup>1</sup>/<sub>2</sub>" diskette, including the following lines (see section 3.1. for the definition of the step designations):

step designation	prescribed displ. $u_z$ (half of the specimen) [mm]	reduction of diameter $\Delta D = 2u_r$ [mm]	reaction force $F$ [N]	$m = 22$		$m = \underline{\hspace{2cm}}$	
				$\sigma_w$ [MPa]	$P_f(\sigma_w)$ [%]	$\sigma_w$ [MPa]	$P_f(\sigma_w)$ [%]
"1"	0.1			-----	-----	-----	-----
"2"	0.2			-----	-----	-----	-----
"3"	0.3			-----	-----	-----	-----
"Pf10% $m_{22}$ "					10	-----	-----
"Pf10%"				-----	-----		10
"Df4"		0.167					
"Df16"		0.212					
"Df10"		0.216					
"Df25"		0.218					
"Df31"		0.248					
"Df28"		0.293					
"Df34"		0.299					

Tab. 7: Results of Task B1: Global quantities: prescribed displacement,  $u_z$ , reduction of diameter,  $\Delta D$ , reaction force,  $F$ , WEIBULL stress,  $\sigma_w$ , and failure probability,  $P_f$  for  $m = 22$ , WEIBULL stress,  $\sigma_w$ , and failure probability,  $P_f$  for determined  $m$ .

10. any other information and comments which the participant considers to be of importance.

If you have made an attempt to characterise the whole sample of the  $N = 32$  specimens with the BEREMIN model (section 3.2.) give information about the following:

11. idea and assumptions you have made to apply the BEREMIN model to all specimens in order to statistically characterise the conditions for cleavage fracture.
12. result of WEIBULL parameter estimation procedure ( $V_0 = 0.001 \text{ mm}^3$ ):

$$m = \underline{\hspace{2cm}}, \sigma_u = \underline{\hspace{2cm}} \text{ MPa}$$

bias correction ( $N = 32$ ):

$$m_{cor} = \underline{\hspace{2cm}}$$

90 % confidence intervals ( $N = 32, \alpha = 0.1$ ):

$$\underline{\hspace{2cm}} \leq m \leq \underline{\hspace{2cm}}, \quad \underline{\hspace{2cm}} \text{ MPa} \leq \sigma_u \leq \underline{\hspace{2cm}} \text{ MPa}$$

## 5. Contact address and deadline

If you have any questions or need any further information please contact

Günter Bernauer  
Institut für Werkstofforschung  
GKSS Forschungszentrum  
Postfach 1160  
D - 21494 Geesthacht  
Phone: ++49 - 4152 - 87 - 2618  
Fax: ++49 - 4152 - 87 - 2625  
e-mail: guenter.bernauer@gkss.de

Please send the results of Task B1 to the address above before

**June 30, 1999**

ASCII data of the graphs and tables should be sent either via e-mail or 3.5" diskette.

## 6. References

- [1] ESIS P 6 98: "Procedure to measure and calculate material parameters for the local approach to fracture using notched tensile specimens", to be issued.
- [2] MUDRY, F. and DiFANT, M.: "A round robin on the measurement of local criteria", IRSID report RI 93.334, September 1993.
- [3] BROCKS, W.: "Numerical round robin on micromechanical models", IWM report T 8/95, Freiburg, 1995.
- [4] BEREMIN, F.M.: "A local criterion for cleavage fracture of a nuclear pressure vessel steel", Metallurgical Transactions A, Vol. 14A (1983), 2277-2287.
- [5] MUDRY, F.: "A local approach to cleavage fracture", Nuclear Engineering and Design 105 (1987), 65-76.
- [6] KHALILI, A. and KROMP, K.: "Statistical properties of WEIBULL estimators", J. Materials Science 26 (1991), 6741-6752.

## Appendix: Equations and parameters of the BEREMIN model for the analysis of cleavage fracture

Based on the weakest link assumption and WEIBULL statistics, the fracture probability of the entire structure follows a two parameter distribution function

$$P_f(\sigma_w) = 1 - \exp\left[-\left(\frac{\sigma_w}{\sigma_u}\right)^m\right] \quad (A1)$$

where

$\sigma_u$  is the scaling factor which describes the point of the distribution function on the stress axis at  $\log 1/(1-P_f) = 0$  or  $P_f = 0.632$ , i.e. 63.2% failure probability;

$m$  is the WEIBULL exponent or WEIBULL modulus which describes the scatter of the distribution.

The WEIBULL stress,  $\sigma_w$ , is defined by a summation of the maximum principal stress,  $\sigma_I$ ,

$$\sigma_w = \sqrt[m]{\sum_{i=1}^{n_{pl}} (\sigma_I^{(i)})^m \frac{V_i}{V_0}} \quad (A2)$$

Since plastic deformations are a prerequisite for cleavage fracture, the summation is taken over the plastically deformed part of the volume, only, i.e. the  $n_{pl}$  elements which have already experienced plastic deformations.

The WEIBULL parameters are  $\sigma_u V_0^{1/m}$  and  $m$ .  $\sigma_u$  itself depends on the choice of the reference volume  $V_0$ . A comparison of WEIBULL distributions is, hence, only admissible for a fixed reference volume.

The evaluation of eq. (A2) can be done in a post-processor programme. The summation over the GAUSS points of an element may be performed before or after putting  $\sigma_I$  to the power  $m$ . In the first case, stresses are linearly averaged within each element. When performing the summation over the volume of the specimen one has to pay attention that the FE model may have unit thickness which may be 1 rad in the axisymmetric case, and may be symmetric to the centre plane. Hence, a respective volume factor has to be applied for the calculation of  $V_i$ .

$\sigma_w$  has to be calculated for every specimen, i.e. at the time step which corresponds to the fracture event of the respective specimen. An interpolation between time steps might be necessary. The correlation between the experimental fracture event and the time step in the FE analysis has to be realised with a monotonically increasing parameter, e.g. the elongation,  $\Delta L$ , or diameter reduction,  $\Delta D$ . If  $N$  specimens have been tested, the relative fracture probability

$$h_j = \frac{j-0.5}{N} \quad (A3)$$

is assigned to the  $j$ -th rank in an ascendingly sequenced sample of the  $N$  specimens. The parameters  $\sigma_u$  and  $m$  in eq. (A1) are to be determined, so that the values of  $P_f$  fit to the

experimental  $h_j$  values best. Since  $\sigma_w$  is dependent on  $m$ , an iterative procedure is necessary to determine  $\sigma_u$  and  $m$ . They can be assessed by the maximum likelihood method [6]. In their investigations, BEREMIN [4] found a value of  $m = 22$  for ferritic pressure vessel steels which may be used as a starting value in the first iteration. If the calculated value of  $m$  deviates from that used in the previous iteration, the procedure is repeated until the difference of two iteration steps,  $\Delta m$ , is less than, e.g., 0.1.

The data are often plotted as <sup>1</sup>

$$y_j = \log \log \left( \frac{1}{1-h_j} \right) \quad \text{vs.} \quad x_j = \log \sigma_w^{(j)} \quad (\text{A4})$$

in order to assure that they follow a WEIBULL distribution, eq. (A1), with sufficient accuracy.

Since the estimation is only based on a sample of size  $N$ , the parameters of the entire population of all possible specimens from the material cannot exactly be determined. Only confidence intervals can be evaluated. A confidence level,  $(1-\alpha)$ , is introduced, which is the required probability that any one estimate will fall within the confidence interval. If the results of the parameter estimation procedure are called  $\sigma_{u0}$  and  $m_0$ , and  $(1-\alpha)$  is the desired confidence level, the following statement about  $m$  and  $\sigma_u$  can be made:

$$\frac{m_0}{l_l} \leq m \leq \frac{m_0}{l_u} \quad (\text{A5})$$

and

$$\sigma_{u0} \exp\left(-\frac{t_l}{m_0}\right) \leq \sigma_u \leq \sigma_{u0} \exp\left(-\frac{t_u}{m_0}\right) \quad (\text{A6})$$

with a probability of at least  $(1-\alpha) \cdot 100$  %.

$l_l$ ,  $l_u$ ,  $t_l$  and  $t_u$  are numbers which only depend on  $N$  and  $\alpha$ . They are listed in Tab. A1 and A2.

If  $m$  is not expressed by a confidence interval, another procedure has to be followed: When going from the sample to the entire population, the parameter  $m$  has to be bias corrected. It will then be denoted  $m_{cor}$ :

$$m_{cor} = m_0 \cdot b \quad (\text{A7})$$

where  $b$  only depends on  $N$ .  $b$  is listed in Tab. A3. This bias correction is important as soon as the WEIBULL parameters shall be applied to other specimens or structures and predictions will be made.

---

<sup>1</sup>log is the natural (Napierian) logarithm.

Confidence level, $1-\alpha$	0,95	0,90	0,80	0,80	0,90	0,95
	Value of $l_u$ for $\alpha/2$			Value of $l_u$ for $1 - \alpha/2$		
N	0,025	0,05	0,10	0,90	0,95	0,975
5	0,604	0,683	0,766	2,277	2,779	3,518
6	0,623	0,697	0,878	2,030	2,436	3,067
7	0,639	0,709	0,785	1,861	2,183	2,640
8	0,653	0,720	0,792	1,747	2,015	2,377
9	0,665	0,729	0,979	1,665	1,896	2,199
10	0,676	0,738	0,802	1,602	1,807	2,070
11	0,686	0,745	0,807	1,553	1,738	1,972
12	0,695	0,752	0,811	1,513	1,682	1,894
13	0,703	0,759	0,815	1,480	1,636	1,830
14	0,710	0,764	0,819	1,452	1,597	1,777
15	0,716	0,770	0,823	1,427	1,564	1,732
16	0,723	0,775	0,826	1,406	1,535	1,693
17	0,728	0,779	0,829	1,388	1,510	1,660
18	0,734	0,784	0,832	1,371	1,487	1,630
19	0,739	0,788	0,835	1,356	1,467	1,603
20	0,743	0,791	0,838	1,343	1,449	1,579
22	0,752	0,798	0,843	1,320	1,418	1,538
24	0,759	0,805	0,848	1,301	1,392	1,504
26	0,766	0,810	0,852	1,284	1,370	1,475
28	0,772	0,815	0,856	1,269	1,351	1,450
30	0,778	0,820	0,860	1,257	1,334	1,429
32	0,783	0,824	0,863	1,246	1,319	1,409
34	0,788	0,828	0,866	1,236	1,306	1,392
36	0,793	0,832	0,869	1,227	1,294	1,377
38	0,797	0,835	0,872	1,219	1,283	1,363
40	0,801	0,839	0,875	1,211	1,273	1,351
42	0,804	0,842	0,877	1,204	1,265	1,339
44	0,808	0,845	0,880	1,198	1,256	1,329
46	0,811	0,847	0,882	1,192	1,249	1,319
48	0,814	0,850	0,884	1,187	1,242	1,310
50	0,817	0,852	0,886	1,182	1,235	1,301
52	0,820	0,854	0,888	1,177	1,229	1,294
54	0,822	0,857	0,890	1,173	1,224	1,286
56	0,825	0,859	0,891	1,169	1,218	1,280
58	0,827	0,861	0,893	1,165	1,213	1,273
60	0,830	0,863	0,894	1,162	1,208	1,267
62	0,832	0,864	0,896	1,158	1,204	1,262
64	0,834	0,866	0,897	1,155	1,200	1,256
66	0,836	0,868	0,899	1,152	1,196	1,251
68	0,838	0,869	0,900	1,149	1,192	1,246
70	0,840	0,871	0,901	1,146	1,188	1,242
72	0,841	0,872	0,903	1,144	1,185	1,237
74	0,843	0,874	0,904	1,141	1,182	1,233
76	0,845	0,875	0,905	1,139	1,179	1,229
78	0,846	0,876	0,906	1,136	1,176	1,225
80	0,848	0,878	0,907	1,134	1,173	1,222
85	0,852	0,881	0,910	1,129	1,166	1,213
90	0,855	0,883	0,912	1,124	1,160	1,206
95	0,858	0,886	0,914	1,120	1,155	1,199
100	0,861	0,888	0,916	1,116	1,150	1,192
110	0,866	0,893	0,920	1,110	1,141	1,181
120	0,871	0,897	0,923	1,104	1,133	1,171

Tab. A1: Confidence factors for  $m$  (also in [1]).

0.26

0.86

Confidence level, $1-\alpha$	0,95	0,90	0,80	0,80	0,90	0,95
N	Value of $t_{\alpha/2}$ for $\alpha/2$			Value of $t_{\beta}$ for $1 - \alpha/2$		
	0,025	0,05	0,10	0,90	0,95	0,975
5	-1,631	-1,247	-0,888	0,772	1,107	1,582
6	-1,386	-1,007	-0,740	0,666	0,939	1,291
7	-1,196	-0,874	-0,652	0,598	0,829	1,120
8	-1,056	-0,784	-0,591	0,547	0,751	1,003
9	-0,954	-0,717	-0,544	0,507	0,691	0,917
10	-0,876	-0,665	-0,507	0,475	0,644	0,851
11	-0,813	-0,622	-0,477	0,448	0,605	0,797
12	-0,762	-0,587	-0,451	0,425	0,572	0,752
13	-0,719	-0,567	-0,429	0,406	0,544	0,714
14	-0,683	-0,532	-0,410	0,389	0,520	0,681
15	-0,651	-0,509	-0,393	0,374	0,499	0,653
16	-0,624	-0,489	-0,379	0,360	0,480	0,627
17	-0,599	-0,471	-0,365	0,348	0,463	0,605
18	-0,578	-0,455	-0,353	0,338	0,447	0,584
19	-0,558	-0,441	-0,342	0,328	0,433	0,566
20	-0,540	-0,428	-0,332	0,318	0,421	0,549
22	-0,509	-0,404	-0,314	0,302	0,398	0,519
24	-0,483	-0,384	-0,299	0,288	0,379	0,494
26	-0,460	-0,367	-0,286	0,276	0,362	0,472
28	-0,441	-0,352	-0,274	0,265	0,347	0,453
30	-0,423	-0,338	-0,264	0,256	0,334	0,435
32	-0,408	-0,326	-0,254	0,247	0,323	0,420
34	-0,394	-0,315	-0,246	0,239	0,312	0,406
36	-0,382	-0,305	-0,238	0,232	0,302	0,393
38	-0,370	-0,296	-0,231	0,226	0,293	0,382
40	-0,360	-0,288	-0,224	0,220	0,285	0,371
42	-0,350	-0,280	-0,218	0,214	0,278	0,361
44	-0,341	-0,273	-0,213	0,209	0,271	0,352
46	-0,333	-0,266	-0,208	0,204	0,264	0,344
48	-0,325	-0,260	-0,203	0,199	0,258	0,336
50	-0,318	-0,254	-0,198	0,195	0,253	0,328
52	-0,312	-0,249	-0,194	0,191	0,247	0,321
54	-0,305	-0,244	-0,190	0,187	0,243	0,315
56	-0,299	-0,239	-0,186	0,184	0,238	0,309
58	-0,294	-0,234	-0,183	0,181	0,233	0,303
60	-0,289	-0,230	-0,179	0,177	0,229	0,297
62	-0,284	-0,226	-0,176	0,174	0,225	0,292
64	-0,279	-0,222	-0,173	0,171	0,221	0,287
66	-0,274	-0,218	-0,170	0,169	0,218	0,282
68	-0,270	-0,215	-0,167	0,166	0,214	0,278
70	-0,266	-0,211	-0,165	0,164	0,211	0,274
72	-0,262	-0,208	-0,162	0,161	0,208	0,269
74	-0,259	-0,205	-0,160	0,159	0,205	0,266
76	-0,255	-0,202	-0,158	0,157	0,202	0,262
78	-0,252	-0,199	-0,155	0,155	0,199	0,258
80	-0,248	-0,197	-0,153	0,153	0,197	0,255
85	-0,241	-0,190	-0,148	0,148	0,190	0,246
90	-0,234	-0,184	-0,144	0,143	0,185	0,239
95	-0,227	-0,179	-0,139	0,139	0,179	0,232
100	-0,221	-0,174	-0,136	0,136	0,175	0,226
110	-0,212	-0,165	-0,129	0,129	0,166	0,215
120	-0,202	-0,158	-0,123	0,123	0,159	0,205

Tab. A2: Confidence factors for  $\sigma_u$  (also in [1]).

N	b	N	b
5	0,700	42	0,968
6	0,752	44	0,970
7	0,792	46	0,971
8	0,820	48	0,972
9	0,842	50	0,973
10	0,859	52	0,974
11	0,872	54	0,975
12	0,883	56	0,976
13	0,893	58	0,977
14	0,901	60	0,978
15	0,908	62	0,979
16	0,914	64	0,980
18	0,923	66	0,980
20	0,931	68	0,981
22	0,938	70	0,981
24	0,943	72	0,982
26	0,947	74	0,982
28	0,951	76	0,983
30	0,955	78	0,983
32	0,958	80	0,984
34	0,960	85	0,985
36	0,962	90	0,986
38	0,964	100	0,987
40	0,966	120	0,990

*Tab. A3: Unbiasing factor for m (also in [1]).*